HISTONE ACETYLATION, NOT STOICHIOMETRY, REGULATES LINKER HISTONE BINDING IN *SACCHAROMYCES CEREVISIAE*

by

Mackenzie Brie Dorothea Lawrence

BSc., The University of Guelph, 2015

A THESIS SUBMITTED IN PARTIAL FULFILLMENT OF
THE REQUIREMENTS FOR THE DEGREE OF

MASTER OF SCIENCE

in

FACULTY OF GRADUATE AND POSTDOCTORAL STUDIES
(Biochemistry and Molecular Biology)

THE UNIVERSITY OF BRITISH COLUMBIA
(Vancouver)

April 2019

COMMITTEE PAGE

The following individuals certify that they have read, and recommend to the Faculty of Graduate and Postdoctoral Studies for acceptance, a thesis/dissertation entitled:

Histone Acetylation, Not Stoichiometry, Regulates Linker Histone Binding in *S. cerevisiae*

submitted by Mackenzie B. D. Lawrence in partial fulfillment of the requirements for

the degree of Master of Science

in Biochemistry and Molecular Biology

Examining Committee:

Dr. LeAnn Howe
Supervisor

Dr. Vivien Measday
Supervisory Committee Member

Supervisory Committee Member

Dr. Peter Stirling
Additional Examiner

Additional Supervisory Committee Members:

Supervisory Committee Member

Supervisory Committee Member

ABSTRACT

Linker histones play a fundamental role in shaping chromatin structure, but how their interaction with chromatin is regulated is not well understood. A combination of genetic and genomic approaches were used to explore the regulation of linker histone binding in the yeast, *Saccharomyces cerevisiae*. We found that increased expression of Hho1, the yeast linker histone, resulted in a severe growth defect, despite only subtle changes in chromatin structure. Further, this growth defect was rescued by mutations that increase histone acetylation. Consistent with this, genome-wide analysis of linker histone occupancy revealed an inverse correlation with histone tail acetylation in both yeast and mouse embryonic stem cells. Collectively, these results suggest that histone acetylation negatively regulates linker histone binding in *S. cerevisiae* and other organisms and provides important insight into how chromatin structure is regulated and maintained to both facilitate and repress transcription.

LAY SUMMARY

Nearly every cell in our body contains a copy of our genome. The genome is encoded by DNA which serves as a blue-print responsible for directing all cellular activities, including growth and proliferation. In order to allow for the packaging of the genome into the nucleus of each cell, DNA is wrapped around proteins referred to as histones. Additional proteins, including another family of histones known as linker histones, bind to the spooled DNA and facilitate compaction of DNA within the cell. Histone proteins can be modified by enzymes which can alter their chemical properties and impact DNA compaction. In this study, we investigated how the binding of linker histones is regulated, specifically examining the role of the histone modification acetylation in mediating this interaction.

PREFACE

This thesis is based on the following first author publication: Lawrence, M. B. D., Coutin, N., Choi, J. K., Martin, B. J. E, Irwin, N. A. T., Young, B., Loewen, C. and Howe, L. J. (2017). Histone Acetylation, Not Stoichiometry, Regulates Linker Histone Binding in *Saccharomyces cerevisiae*. *Genetics*, 207(1), 347-355. Experiments were designed by Dr. LeAnn Howe, Dr. Jennifer Choi, Nicolas Coutin and Mackenzie Lawrence. Dr. Jennifer Choi conducted the SGA screen and Nicolas Coutin conducted the Hho1 ChIP-sequencing experiments. The subsequent data analysis and all other experiments were conducted by Mackenzie Lawrence.

TABLE OF CONTENTS

LIST OF TABLES

LIST OF FIGURES

LIST OF ABBREVIATIONS

α	Alpha; signifies anti
Δ	Delta; signifies deletion
°C	Degree Celsius
ac	Acetyl
ATP	Adenosine triphosphate
bp	base pair
BSA	Bovine serum albumin
ChIP	Chromatin immunoprecipitation
ChIP-QPCR	ChIP-quantitative PCR
ChIP-seq	ChIP-sequencing
CTD	C-terminal domain
C-terminal	Carboxy-terminal
D. melanogaster	*Drosophila melanogaster*
DNA	Deoxyribonucleic acid
Esa1	Essential SAS2-related acetyltransferase 1
EDTA	Ethylenediaminetetraacetic acid
Gcn5	General control non-derepressible 5
GEO	Gene Expression Omnibus
H2AS129	Histone H2A serine 129
H3K4	Histone H3 lysine 4
H3K9	Histone H3 lysine 9
H3K14	Histone H3 lysine 14
H3K18	Histone H3 lysine 18
H3K20	Histone H3 lysine 20
H3K23	Histone H3 lysine 23
H3K36	Histone H3 lysine 36
H3K56	Histone H3 lysine 56

H3K79	Histone H3 lysine 79
H3S10	Histone H3 serine 10
H4K5	Histone H4 lysine 5
H4K8	Histone H4 lysine 8
H4K12	Histone H4 lysine 12
H4K16	Histone H4 lysine 16
H4R3	Histone H4 arginine 3
HA	Hemagglutinin
HAT	Histone acetyltransferase
HDAC	Histone deacetylase complex
Hho1	Histone H1
K	Lysine
me	Methyl
MNase	Micrococcal nuclease
NET-seq	Native elongation transcript-seq
NCP	Nucleosome core particle
NFR	Nucleosome free region
NTD	N-terminal domain
NuA3	Nucleosome acetyltransferase for histone H3
NuA4	Nucleosome acetyltransferase for histone H4
OD_{600}	Optical density, at 600nm
ORF	Open reading frame
PCR	Polymerase chain reaction
PHD	Plant homeodomain
PBS-T	Phosphate buffered saline with tween
PHD	Plant homeodomain
PTM	Post-translational modification
Q	Glutamine
R	Arginine

rDNA	Ribosomal DNA
RNA	Ribonucleic acid
RNAPII	RNA polymerase II
Rpd3	Reduced potassium dependency 3
Rpd3L	Rpd3 large complex
Rpd3S	Rpd3 small complex
rpm	Rotations per minute
RSC	Remodels structure of chromatin
Rtt109	Regulator of Ty1 transposition 109
S. cerevisiae	*Saccharomyces cerevisiae*
SAGA	Spt-Ada-Gcn5-acetyltransferase
SAM	S-adenosyl methionine
SDS	Sodium dodecyl sulfate
SDS-PAGE	Sodium dodecyl sulfate-polyacrylamide gel electrophoresis
SGA	Synthetic genetic array
STORM	Stochastic optical reconstruction microscopy
SWI/SNF	Switching/sucrose non-fermenting
TE	Tris-EDTA
TSS	Transcription start site
YEATS	Yaf9-ENL-AF9-Taf14-Sas5

CHAPTER 1 – INTRODUCTION

1.1 Chromatin

DNA

All living cells contain genetic information in the form of deoxyribonucleic acids (DNA), necessary for growth and proliferation. DNA molecules are long polymers composed of covalently linked nucleotides. Within cells, DNA does not usually exist as a single molecule, rather two strands of anti-parallel DNA form a double helical structure that can be copied, allowing for genome duplication. These DNA molecules contain distinct series of nucleotides called genes, which encode for proteins. The haploid human genome is composed of approximately 3.2 billion base pairs (bp) and encodes more than 20,000 protein-coding genes (Human Genome Sequencing Consortium 2004). In order to facilitate the compaction of DNA into the nucleus of the cell, DNA is packaged into chromatin.

Histones

Chromatin is a dynamic structure composed of DNA, histones and non-histone proteins. The basic repeating unit of chromatin is the nucleosome core particle (NCP), which is composed of 147 bp of DNA wrapped 1.7 times around an octamer of core histones H2A, H2B, H3 and H4 (van Holde 1989; Luger *et al.* 1997). A fifth protein, termed the "linker histone", binds the nucleosome dyad, interacting with the DNA entering and exiting the nucleosome (Syed *et al.* 2010; Meyer *et al.* 2011; Zhou *et al.* 2013; 2015b; Bednar *et al.* 2017). The binding of the linker histone wraps an additional 20 bp of DNA around the NCP,

completing the super-helical turns forming a structure known as the chromatosome (Allan *et al.* 1980; Thoma and Koller 1981; Zhou *et al.* 1998). Nucleosomal arrays are folded into higher-order chromatin fibres, compacting DNA further (Luger and Richmond 1998). In order to regulate gene expression and other DNA-templated processes, chromatin is dynamically and reversibly altered to allow access of the cellular machinery to the underlying DNA.

The core histones are highly conserved, basic proteins that comprise the major architectural proteins of chromatin. They contain three distinct structural domains, a long, hydrophilic N-terminal tail, a globular hydrophobic core and a short, hydrophobic C-terminus (Arents and Moudrianakis 1995; Luger and Richmond 1998). The bulk of the histone protein mass is comprised of the globular core, which contains the highly conserved structural motif, termed "the histone fold" (Arents and Moudrianakis 1995). The histone fold, which consists of 3 α-helices separated by 2 loops (Luger *et al.* 1997), forms an extensive protein-protein interface important for histone heterodimerization (Arents *et al.* 1991; Arents and Moudrianakis 1993). The N-terminal tails of the core histones protrude from the surface of the nucleosome and are targets for post-translational modifications (PTMs) (Luger *et al.* 1997; Morales and Richard-Foy 2000). H2A is the only canonical core histone with a flexible C-terminal tail. The C-terminal tail of H2A protrudes from the NCP at the dyad axis (Luger *et al.* 1997) and is primarily responsible for the interactions at the interface between the H3-H4 tetramer and H2A-H2B dimers (Suto *et al.* 2000).

The core histones are synthesized primarily during S phase of the cell cycle, and incorporated into chromatin in a replication-dependent manner (Spalding *et al.* 1966; Borun *et al.* 1967). In humans this includes H2A, H2B, H3.1, H3.2 and H4, while the budding yeast, *Saccharomyces cerevisiae* (*S. cerevisiae*) has a single canonical H3, in addition to H2A, H2B and H4. Multiple copies of the core histone genes are located in several histone gene clusters in the mammalian and yeast genomes (Marzluff *et al.* 2002; Eriksson *et al.* 2012). In addition to the core histones that form the canonical nucleosome, non-allelic histone variants also exist. Histone variants are synthesized throughout the cell cycle and are incorporated into chromatin in a replication-independent manner. In most cases, only single copies of variant genes are found throughout an organisms' genome (Marzluff *et al.* 2002; Eriksson *et al.* 2012). In humans, 13 core histone variants, including 2 testis-specific variants have been identified (for reviews see: Kamakaka and Biggins 2005; Sarma and Reinberg 2005; Talbert and Henikoff 2010; Maze *et al.* 2014). However, *S. cerevisiae* only contains two core histone variants, the H2A variant HTZ1 and the centromeric H3 variant, CSE4.

Higher order packing and DNA accessibility

Different levels of chromatin compaction exist within the nucleus. Highly compact chromatin is often referred to as heterochromatin. Chromosomal regions that contain a high density of repetitive DNA elements, including clusters of satellite sequences and transposable elements, are targets for heterochromatin formation (Lohe *et al.* 1993). In

many organisms, heterochromatin is found in the telomeres and in the domains surrounding centromeres of chromosomes, referred to as centromeric heterochromatin. These regions often remain condensed throughout the cell cycle. In contrast, euchromatin is a lightly packed form of chromatin that encompasses all non-heterochromatic regions of the genome. Euchromatin decondenses during interphase of the cell cycle and contains the majority of genes that encode for cellular proteins. Unlike mammals, the majority of the genome of the budding yeast, *S. cerevisiae* is composed of euchromatin. However, several regions of the genome are silenced or can be silenced, including the two silent mating-type loci, HMR and HML, telomeres and ribosomal RNA-encoding DNA (rDNA) (Weiss and Simpson 1998; Ravindra *et al.* 1999; Rusche *et al.* 2003). The formation of chromatin facilitates the packaging of DNA into the nucleus of cells, however, it also represents a significant physical barrier to transcription, DNA replication and repair.

Several mechanisms exist to regulate chromatin structure within the cell. Firstly, sliding and restructuring of nucleosomes is accomplished by chromatin remodelers, large multi-subunit, ATP-dependent enzymes. Secondly, the post-translational modification (PTM) of DNAs and histones can alter chromatin dynamics. Lastly, the incorporation of non-canonical histone variants can also modify chromatin structure by altering nucleosome stability and existing patterns of histone PTMs. These mechanisms allow for regulation of chromatin condensation and DNA accessibility.

1.2 Histone Post-Translational Modifications

The post-translation modification (PTM) of histone proteins is one mechanism by which chromatin structure can be dynamically regulated. Histone PTMs can directly alter chromatin structure by disrupting histone-DNA contacts, or indirectly by modulating the recruitment and binding of chromatin modifying factors (for review see: Bannister and Kouzarides 2011). The majority of histone PTMs occur on the highly conserved histone N-terminal tails which protrude away from the nucleosome core (Luger *et al.* 1997; Strahl and Allis 2000). To date, a wide variety of histone modifications and sites have been identified including lysine acetylation, lysine and arginine methylation, serine phosphorylation and lysine ubiquitylation (Murray 1964; Allfrey *et al.* 1964; Stevely and Stocken 1966; Hunt and Dayhoff 1977; Zhao and Garcia 2015). Numerous studies have shown that histone PTMs are correlated with diverse cellular processes, including gene activation (Cheung et al., 2000), heterochromatic gene silencing (Rea et al., 2000), DNA replication (Vogelauer et al., 2002) and DNA damage responses (van Attikum and Gasser, 2005). However, despite the potential for combinatorial complexity of histone modifications, only a small number of states are actually observed *in vivo* (Liu *et al.* 2005a; Wang *et al.* 2008). Understanding how histone PTM mediate chromatin structure and dictate biological outcomes remains a major of focus in the field.

1.3 Histone Acetylation

Histone acetylation is one of the most widely studied histone PTMs. It was first described in 1963 and was subsequently shown to be important for regulating ribonucleic acid (RNA) expression *in vitro* (Phillips 1963; Allfrey *et al.* 1964). This led to the proposal that histone acetylation was a dynamic and reversible modification, important for regulating gene expression. Indeed, various studies have demonstrated a clear correlation between histone acetylation and gene expression *in vivo* (Gershey *et al.* 1968; Hebbes *et al.* 1988). Since its initial discovery, numerous acetylation sites have been identified and a tremendous amount of work has been done to elucidate the regulation and functional consequences of histone acetylation.

HATs and HDACs

Histone acetylation is maintained by the competing activities of two groups of enzymes. Histone acetyltransferases (HATs) catalyze the addition of a single acetyl moiety to the ε-amino group of lysine residues (DeLange et al. 1969; Millar and Grunstein 2006) and histone deacetylases (HDACs) catalyze their removal (Taunton et al. 1996). Acetylation occurs primarily on histone N-terminal tails, however, the globular domains and C-terminal domain of H2A can also be acetylated (Zhang et al. 2003; Valero et al. 2016). Numerous HATs have been identified, many of which are components of large multi-subunit complexes that contain auxiliary domains important for enzymatic activity and targeting (Table 1.1) (Struhl 1998). Although many recombinant HAT proteins can acetylate free histones, often nucleosomal acetylation occurs only in the context of the *in vivo* HAT

complexes. Moreover, incorporation of HATs into complexes often alters substrate specificity. For example, Gcn5 which was first identified in yeast as a transcriptional co-activator (Georgakopoulos and Thireos 1992) and later shown to have HAT activity (Brownell et al. 1996), is a component of the Ada, SLIK/SALSA, HAT-A2 and SAGA complexes (Grant *et al.* 1997; Sendra *et al.* 2000; Pray-Grant *et al.* 2002). While recombinant Gcn5 preferentially acetylates histone H3K14, it can also acetylate residues on histone H4 (Kuo *et al.* 1996). However, within the Ada and SAGA complexes, Gcn5 acetylates nucleosomal H3 and H2B, but not histone H4 (Grant *et al.* 1997; 1999; Suka *et al.* 2001; Jiang *et al.* 2007). Similarly, Sas3 alone acetylates free histones, while the Sas3-containing NuA3 HAT complex acetylates nucleosomal histone H3 at some of the same residues as the Gcn5-containing HATs, in addition to distinct H3 targets (Takechi and Nakayama 1999; John *et al.* 2000; Howe *et al.* 2001). Like HATs, many HDACs are also catalytic subunits of multi-protein complexes (Table 1.2). Some of these complexes have broad and overlapping substrate specificities, while others act at specific lysine residues. For example, Rpd3 can exist in both the Rpd3S and RpdL complexes, which together deacetylate nearly all sites on histones H2A, H2B, H3 and H4 (Rundlett et al. 1996; Zhou et al. 2009). In contrast, Hda1 deacetylates lysine residues on histones H2B and H3 (Wu et al. 2001). Together, HATs and HDACs reversibly modify histones and play a role in mediating chromatein dynamics.

Table 1.1: Histone lysine acetyltransferases in *S. cerevisiae* and known substrates

Catalytic Enzyme	Complex	Substrate
Gcn5	SAGA	H2B, H3 tails
Gcn5	SLIK	H2B, H3 tails
Gcn5	ADA	H3 tails
Gcn5	HAT-A2	H3 tails
Hat1	HATB	H2A, H4 tails
Esa1	NuA4	H2A, H4 tails
Esa1	Pic NuA4	H2A, H4 tails
Sas2	SAS	H4 tails
Sas3	NuA3	H3 tails
Rtt109	Rtt109-Vps75	H3(K56), tails

Table 1.2: Histone lysine deacetylases in *S. cerevisiae* and known substrates

Catalytic Enzyme	Substrate
Hda1	H2B, H3 tails
Hos1	H2B tails
Hos2	H4 tails
Hos3	H2B, H4 tails
Hst1	H3 tails
Hst3	H3(K56)
Hst4	H3(K56)
Rpd3	H2A, H2B, H3, H4 tails
Sir2	H3, H4 tails

Targeting

Histone acetylation is typically associated with actively transcribed genes. Acetylation occurs primarily at promoter regions, however, some acetylation marks are localized throughout the bodies of transcribed genes (Pokholok *et al.* 2005; Liu *et al.* 2005b; Weiner *et al.* 2015). Promoter-targeted acetylation plays a role in transcription initiation. In yeast, this is accomplished by the interaction of the HAT complexes, SAGA (Gcn5) and NuA4 (Esa1) with transcriptional activators, which promotes the recruitment of the basal transcription machinery required for transcription initiation (Bhaumik and Green 2002). Acetylation is also targeted to gene bodies by several different mechanisms. Firstly, various HATs are localized to transcribed regions through interactions with the phosphorylated CTD of RNAPII, including NuA4 (Esa1) (Ginsburg *et al.* 2009) and SAGA (Gcn5) (Govind *et al.* 2007) in yeast and PCAF in humans (Obrdlik *et al.* 2008). HATs are also recruited to gene bodies through H3K4 and K36 methylation. The histone methyltransferases responsible for modifying these histone residues associate with elongating RNAPII, creating a trail of methylation which can serve as docking sites for HATs (Shi *et al.* 2006; Martin *et al.* 2006; Shi *et al.* 2007). Lastly, acetylated histones can also be incorporated into chromatin at promoter and transcribed regions via histone turnover (Dion *et al.* 2007; Rufiange *et al.* 2007).

Histone hypoacetylation is often associated with repressed chromatin and inactive genes. In yeast, at least 9 HDACs have been identified, which preferentially deacetylate particular sets of genes and regions of the genome (Table 1.2) (Robert *et al.* 2004; Li *et al.* 2013).

Several of these HDACs are recruited to promoter regions, where they are thought to play a role in repressing transcription. For example, Rpd3L is targeted to promoter regions via the transcriptional repressor, Ume6 (Kadosh and Struhl 1997; Rundlett *et al.* 1998). Another way that HDACs are thought to be targeted to promoter regions is via association with the Tup1-Ssn6 co-repressor complex, which interacts with sequence specific transcriptional repressors (Davie *et al.* 2003; Malavé and Dent 2006). In addition to preferentially deacetylating promoters, HDACs also function throughout gene bodies. For example, Rpd3S is targeted to actively transcribed genes through association with di- and tri-methylated H3K36, resulting in deacetylation from the mid to 3' end of genes (Carrozza *et al.* 2005; Joshi and Struhl 2005; Li *et al.* 2009; Drouin *et al.* 2010). This form of HDAC targeting is thought to restore chromatin structure in the wake of elongating RNAPII, preventing cryptic transcription along gene bodies (Carrozza *et al.* 2005; Li *et al.* 2009).

Impact on chromatin structure

Histone acetylation is thought to contribute to the opening of chromatin structure through a variety of mechanisms. For example, histone acetylation neutralizes the positively charged lysine residues in the N-terminal tails, reducing their affinity for the negatively charged phosphate backbone of DNA (Hong *et al.* 1993; Lee *et al.* 1993). Although acetylated nucleosomes do not undergo large structural changes, they exhibit decreased thermal and salt stability and increased unwrapping of the outer-turn of nucleosomal DNA, particularly the linker DNA (Ausió and Van Holde 1986; Li *et al.* 1993; Gansen *et al.* 2009; Wakamori *et al.* 2015). Numerous studies have also shown that histone acetylation results

in the decompaction of higher-order chromatin fibres, with H2B and H4 acetylation playing the largest role in unfolding (Norton *et al.* 1989; Tse *et al.* 1998; Shogren-Knaak 2006; Wang and Hayes 2008; Robinson *et al.* 2008; Allahverdi *et al.* 2011; Wakamori *et al.* 2015). Thus, histone acetylation can directly regulate both the structure of individual nucleosomes and chromatin fibers, increasing the accessibility of regulatory proteins to chromatin templates.

Histone acetylation can also regulate chromatin structure indirectly by mediating the recruitment and binding of chromatin modifying factors. For example, several families of protein domains have been identified with specificity for acetylated lysine residues, including bromodomains (Dhalluin *et al.* 1999), YEATS (Le Masson *et al.* 2003) (Li *et al.* 2014), double PHD (Zeng *et al.* 2010) and double PH domains (Su *et al.* 2012). The most well-characterized of these are the bromodomains, which are found in a wide range of nuclear proteins, including many HATs, transcriptional regulators and chromatin remodelers (Dhalluin *et al.* 1999; Filippakopoulos *et al.* 2012). For example, the Gcn5 bromodomain can bind to various acetyl-lysine residues on histone H3 and H4 and is thought to be important for stimulating HAT activity (Owen 2000; Hudson *et al.* 2000; Cieniewicz *et al.* 2014). Many chromatin remodelers, including RSC and SWI/SNF in yeast contain numerous bromodomains that have been shown to promote efficient anchoring and remodeling activity of acetylated nucleosomes (Kasten *et al.* 2004; Hassan *et al.* 2007). Lastly, histone acetylation can also block the activity of various chromatin-associated proteins. For example, H3K14ac has been shown to negatively regulate the activity of the

chromatin remodeler ACF (Shogren-Knaak *et al.* 2006) and also block the activity of the H3K4 demethylase, Jhd2 (Maltby *et al.* 2012a). Therefore, histone acetylation can indirectly regulate chromatin structure and transcription through interactions with numerous chromatin modifying proteins.

1.4 Linker Histones

Metazoan linker histones

Linker histones belong to a distinct histone protein family and are present in most eukaryotic cells. Unlike the highly conserved core histones, linker histones exhibit much greater sequence variability. Despite this, metazoan linker histones share a three-domain structure consisting of a short N-terminal tail, a central globular domain and a long, basic C-terminal tail (Allan et al. 1980). The globular domain has a winged-helix fold structure that is conserved from yeast to humans (Ramakrishnan et al. 1993) and is necessary for generating the 168 bp chromatosome particle, resulting from micrococcal nuclease (MNase) digestion of native chromatin (Figure 1.1) (Singer and Singer 1976; Allan et al. 1980; Patterton et al. 1998; Zhou et al. 2013). The N- and C-terminal domains are less conserved and account for the majority of sequence heterogeneity between the H1 subtypes (Ponte 2003). No significant role in chromatin binding and condensation has been identified for the N-terminal domain (NTD), however, it has been proposed that the NTD may assist in targeting and anchoring the globular domain to the nucleosome (Allan et al. 1980; 1986). Further, extensive PTM sites on the NTD suggest that it serves as a binding

platform for other proteins (Wiśniewski *et al.* 2007; Review: Godde and Ura 2008). The highly basic CTD is intrinsically disordered in aqueous solution, however, in the presence of tetrahedral anions and DNA it adopts considerable α-helical character (Clark et al. 1988; Ali et al. 2004a). Concomitant with the ability of the CTD to bind negatively charged species, its primary role is to stabilize the folding of nucleosomal arrays into chromatin fibers via neutralizing the charge of the linker DNA (Allan et al. 1986; Clark and Kimura 1990; Carruthers et al. 1998; Misteli et al. 2000; Hendzel et al. 2004). Further, the CTD is required for higher-affinity binding of H1 to chromatin (Zhou et al. 2013). This three-domain structure is found in complex eukaryotes, however, some protists have a linker histone that more closely resemble only the C-terminal tail of the H1 linker histones (for review see: Kasinsky *et al.* 2001).

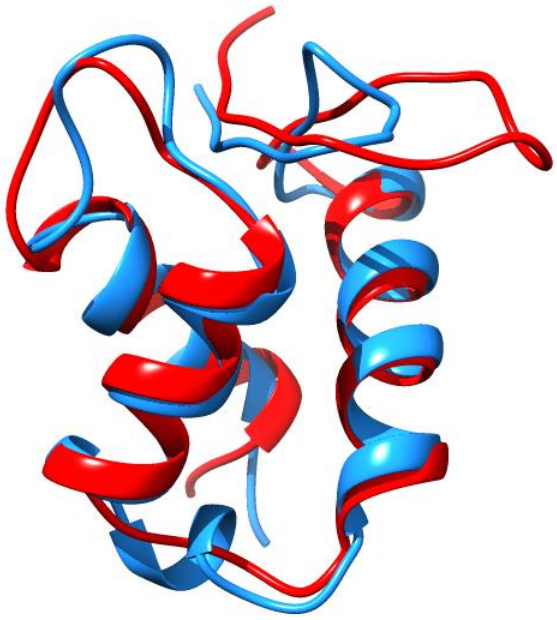

Figure 1.1: Structural comparison of the globular domains of human H1.0 and yeast Hho1
Phyre2 was used to model human H1.0 (NP_005309) (blue) and the average NMR ensemble of the first globular domain was used to for Hho1 (PDB: 1UST) (red). Structures were superimposed using the MatchMaker tool in Chimera (Ali et al. 2004b; Pettersen et al. 2004; Kelley et al. 2015).

Linker histones form a large and diverse family of proteins. In mice and humans, 11 linker histone subtypes have been identified, including seven somatic subtypes (H1.1-H1.5, H1.10 and H1.0), three testis-specific subtypes (H1.6, H1.7 and H1.9) and one oocyte-specific subtype (H1.8) (Happel and Doenecke, 2009). Of the somatic linker histones, H1.1 to H1.5 are expressed in a replication-dependent manner, while H1.10 and H1.0 are replication-independent and can be expressed in non-proliferating cells (Happel et al. 2009). H1.1 to H1.5 and H1.10 are ubiquitously expressed, while H1.0 accumulates in terminally differentiated cells (Zlatanova and Doenecke 1994; Happel et al. 2009). In accordance with this expression pattern, H1.0 in amphibians and birds (referred to as H5) is associated with

highly condensed, transcriptionally inert chromatin characteristic of terminally differentiated cells, such as nucleated erythrocytes (Coles et al. 1987; Koutzamani et al. 2002). Lastly, *Drosophila melanogaster* expresses two linker histone subtypes, one somatic and one germline subtype, known as BigH1, named for its extended N-terminal tail (Lifton et al. 1978; Pérez-Montero et al. 2013). The presence of multiple histone-encoding genes in many metazoans has made studying the functional roles of linker histones *in vivo* challenging.

Yeast linker histone, Hho1

Although linker histones were first described in mammals in the early 1950s (Stedman and Stedman 1951), no bona fide linker histone had been identified in budding yeast, leading some researchers to suggest that yeast lacked a linker histone (Shen et al. 1995). However, in the 1990s shortly after the yeast genome was sequenced, a putative linker histone, termed Hho1 was discovered (Landsman 1996; Ushinsky et al. 1997; Patterton et al. 1998). The structure of Hho1 varies from that of metazoan linker histones. Hho1 contains a short NTD, globular domain and unlike metazoan linker histones, a second globular domain connected by a linker with similar sequence and composition as the C-terminal domain of canonical histone H1 (Landsman 1996; Ushinsky et al. 1997; Ali et al. 2004b). Studies have shown that both globular domains can fold into similar structures, however, despite sharing ~43% sequence identity, they have considerably different stabilities (Ono et al. 2003; Ali et al. 2004b). This lead researchers to suggest that Hho1 could simultaneously bind two nucleosomes at once (Schäfer et al. 2005). However, similar to the CTD of

canonical histone H1, the second globular domain of Hho1 is thought to be largely unstructured under physiological conditions and similarly adopts helical content in the presence of tetrahedral anions (Ono et al. 2003; Ali et al. 2004b). Additionally, Hho1 was shown to form a stable ternary complex with di-nucleosomes *in vitro* at similar ratios of linker histone-to-nucleosome found in more complex eukaryotes (Patterton et al. 1998). Moreover, while the first globular domain of Hho1 is sufficient for generating the 168 bp chromatosome upon MNase digestion (Patterton et al. 1998), the second globular domain is not (Ali and Thomas 2004). Lastly, another study investigating the role of Hho1 in transcriptional silencing found that mutant Hho1 lacking the second globular domain was able to recapitulate the phenotype of full length Hho1 under various conditions (Yu et al. 2009). Thus, Hho1 is thought to interact with nucleosomes in a similar fashion as metazoan linker histones.

Linker histone stoichiometry and nucleosome repeat length

One proposed mechanism for regulating linker histone binding is through the alteration of linker histone abundance. Linker histone abundance varies across species and between cell types. For example, vertebrate cells, which have many gene-poor regions, express approximately 1 molecule of linker histone for every nucleosome and this varies by cell type (Woodcock et al. 2006). Studies in various mouse tissues have determined ratios of 0.79 in splenocytes, 0.83 in thymocytes, 0.79 in adult hepatocytes, 0.76 in neonatal hepatocytes and 0.50 in embryonic stem (ES) cells (Fan et al. 2003; 2005b). Transcriptionally inert avian erythrocytes express 1.3 linker histones per nucleosome

(Bates and Thomas 1981; Coles et al. 1987). In *S. cerevisiae*, linker histone abundance is much lower than that observed in other eukaryotes, consistent with the gene-dense nature of this yeast's genome. Downs et al. (2003) estimated linker histone stoichiometry in yeast to be one molecule for every 4 nucleosomes, while data from Freidkin and Katcoff (2001) suggested it is much lower, at one molecule of Hho1 for every 37 nucleosomes. Two high throughput analyses of protein expression in yeast have estimated that there are 2610 and 6560 molecules of Hho1 per haploid cell, representing ratios of 1:26 and 1:10 for the ~68,000 annotated nucleosomes in yeast (Ghaemmaghami et al. 2003; Brogaard et al. 2012; Kulak et al. 2014). Interestingly, there tends to be a linear relationship between the ratio of linker histone to nucleosome and the nucleosome repeat length (NRL) (Woodcock et al. 2006).

The NLR is the average distance between the centres of neighbouring nucleosomes. It is an important physical property of chromatin and depends on the length of the linker DNA. One of the primary roles of linker histones, which contain a high proportion of positively charged residues, is to neutralize the charge of DNA. Thus, when the amount of linker histones per nucleosome is reduced, charge homeostasis can be restored by decreasing nucleosome spacing (Woodcock et al. 2006). In eukaryotes, NRLs exhibit a wide variety of values ranging from 165 bp in *S. cerevisiae*, to 175–190 bp for most vertebrate cells and tissues (van Holde 1989; Woodcock et al. 2006). It is thought that the differences in NRL in yeast are due to the fact that yeast have sub-stoichiometric levels of linker histones compared to other eukaryotes. Indeed studies in mouse, where up to three somatic H1

subtypes were knocked out in different tissues resulting in a 50% reduction in H1 levels, showed a consistent decrease in NRL (Fan et al. 2003; 2005b). In accordance, increased linker histone stoichiometry should result in longer NRLs. This was shown by Gunjan et al. (1999) upon overexpression H1.0 and H1.3 in cultured mouse fibroblasts, resulting in a 1.2–1.4 fold increase in total H1 and an increase in NRL of ~15 bp. Moreover, the NRL of newly replicated chromatin in HeLa cells has an NRL of ~165 bp, similar to values reported for mouse embryonic stem (ES) cells and yeast (Smith et al. 1984; Woodcock et al. 2006).

Impact on chromatin

Linker histones are important factors that mediate chromatin structure. The precise location of the linker histone within the chromatosome and how this contributes to higher-order folding are long-standing questions in the field. Linker histones bind to nucleosomes at the dyad, interacting with linker DNA at the entry and exit sites of the nucleosome (Syed *et al.* 2010; Meyer *et al.* 2011; Zhou *et al.* 2013; 2015b; Bednar *et al.* 2017). Binding occurs primarily through interactions of positively charged lysine and arginine residues in globular and C-terminal domains with nucleosomal and linker DNA, respectively (Allan *et al.* 1980; 1986; Duggan and Thomas 2000; Brown *et al.* 2006; Zhou *et al.* 2015b; Bednar *et al.* 2017). Various on- and off-dyad binding modes have been reported, and substitutions at key residues within the globular domain are thought to be important for determining the mode of binding of different linker histone subtypes (Zhou *et al.* 2015b; 2016). Moreover, different binding modes have been associated with distinct structural states *in vitro*, which may be related to specific chromatin functions (Song *et al.* 2014; Zhou *et al.* 2015b).

However, considerably less is known regarding the role of the N- and C-terminal domains of H1 within the chromatosome or how PTMs may affect the interaction and structures of these domains. Moreover, exactly how linker histones mediate higher-order chromatin folding *in vivo* remains unclear.

Early studies examining the role of linker histones in chromatin condensation showed that loss of linker histones resulted in morphological changes in chromatin fibres under different salt conditions (Thoma *et al.* 1979). Since then, linker histones have been shown to play an important role in the formation of the 30 nm fibre and higher-order structure *in vitro* (Finch and Klug 1976; Thoma *et al.* 1979; Robinson *et al.* 2006). However, the existence of the 30 nm fibre and its relevance *in vivo* is still debated (for reviews see: Robinson and Rhodes 2006; Maeshima *et al.* 2010). More recently, an *in vivo* study using stochastic optical reconstruction microscopy (STORM) to visualize chromatin structure was performed (Ricci *et al.* 2015). Chromatin fibres were visualized at the single-cell level in variety of cell types during interphase, with a resolution of ~20 nm. It was found that nucleosomes are arranged into discrete heterogeneous domains along the chromatin fibre, termed "nucleosome clutches" (Ricci *et al.* 2015). Interestingly, differentiated human fibroblast contained larger clutches compared to mouse ES cells. Additionally, larger clutches with higher nucleosome density and linker histone levels correlated well with heterochromatin markers (Ricci *et al.* 2015). These findings confirm the role of linker histones in chromatin condensation, while suggesting that *in vivo* 30 nm structures may only exist as short fragments, rather than long continuously folded fibres (Ricci *et al.* 2015).

Although there are numerous outstanding questions regarding the precise role of linker histones in chromatin organization, linker histones are thought to interact with both nucleosomes and chromatin to facilitate the formation of higher-order structures.

Impact on transcription

Regardless of the exact organization of folded H1-containing chromatin, because linker histones limit DNA accessibility and promote chromatin compaction, they are thought to be general repressors of transcription (Bustin *et al.* 2005; Happel and Doenecke 2009). Thus, regulating their interaction with chromatin may provide a means to control access of the transcriptional machinery to DNA. Indeed, genome-wide studies of various linker histone subtypes have shown a non-uniform distribution of linker histones across the genome, with a characteristic binding pattern in which H1 occupancy is reduced over promoter regions primarily at actively transcribed genes (Cao *et al.* 2013; Izzo *et al.* 2013; Nalabothula *et al.* 2014; Millán-Ariño *et al.* 2014). Additionally, different H1 subtypes also exhibit differential binding preferences in somatic cells and during cellular differentiation. For example, the distribution of H1.5 differs in human ES cells compared to differentiated fibroblasts, demonstrating a unique role for H1.5 in chromatin condensation in differentiated cells (Li *et al.* 2012). Cao *et al.* (2013) also show that H1.3 and H1.2 in mouse ES cells show very similar distributions, however, they also exhibit differences in binding specificities. Interestingly, altering linker histone levels *in vivo* results in both up and down regulation of specific genes. In yeast, deletion of non-essential Hho1 actually resulted in decreased expression at a small subset of genes (Hellauer *et al.* 2001). Similarly, in mouse

ES cells with H1 gene knock-downs resulting in a 50% reduction in total H1 levels, only a small subset of genes were up or down regulated compared to wild type cells (Fan *et al.* 2005a). Together, this suggests that specific linker histone subtypes may play a role in fine-tuning gene expression rather than acting as general repressors of transcription.

1.5 Summary of Research Hypotheses

Linker histones limit DNA accessibility and promote chromatin compaction, therefore, regulating their interaction with chromatin may provide a means to control access of the transcriptional machinery to DNA. One proposed mechanism for regulating linker histone binding is through the alteration of linker histone abundance. *S. cerevisiae* expresses one molecule of linker histone for every 4–37 nucleosomes (Freidkin and Katcoff 2001; Downs *et al.* 2003), consistent with the gene-dense nature of this yeast's genome. In contrast, vertebrate cells, which have many gene-poor regions, express approximately 1 molecule of linker histone for every nucleosome and transcriptionally inert avian erythrocytes express 1.3 linker histones per nucleosome (Woodcock *et al.* 2006). However, several studies have demonstrated that linker histone occupancy is not uniform across the genome of a given cell type, suggesting that factors in addition to protein abundance regulate linker histone binding. For example, the yeast linker histone, Hho1, cross-links poorly to the first nucleosome relative to the transcription start site (TSS) and is instead enriched in regions with increased nucleosome spacing (Rhee *et al.* 2014; Ocampo *et al.* 2016). Further, transcriptionally active regions tend to be depleted in linker histones in multiple organisms

(Schafer *et al.* 2008; Cao *et al.* 2013; Izzo *et al.* 2013; Millán-Ariño *et al.* 2014; Ocampo *et al.* 2016).

One potential mechanism for regulating linker histone binding is via histone acetylation, which is enriched on active genes. Because linker histones bind to nucleosomes via contacts with DNA as it enters and exits the nucleosome, acetylation, which promotes DNA unwrapping, could disrupt Hho1 binding sites (Neumann *et al.* 2009; Syed *et al.* 2010; Simon *et al.* 2011; Meyer *et al.* 2011; Zhou *et al.* 2013; 2015a; Kim *et al.* 2015; Ikebe *et al.* 2016; Bednar *et al.* 2017). Indeed, others have observed increased linker histone mobility in cells treated with histone deacetylase inhibitors (Raghuram *et al.* 2010). Despite this evidence, however, the regulation of linker histone binding by core histone acetylation has not been thoroughly explored.

In this study, we designed a novel scheme to determine linker histone stoichiometry in yeast and investigated the impact of *HHO1* overexpression on chromatin structure. Our data suggest that linker histone stoichiometry in yeast is one molecule of Hho1 for every 19 nucleosomes. Moreover, we show that increasing Hho1 levels results in a severe growth defect, despite only modestly impacting Hho1 occupancy or gross chromatin structure. Hho1 toxicity could be rescued by increased histone acetylation, consistent with the negative correlation between linker histone stoichiometry and histone acetylation in both yeast and mouse embryonic stem cells. Collectively these results suggest that factors in

addition to linker histone stoichiometry, including histone acetylation, dictate the impact that linker histones have on chromatin structure.

CHAPTER 2 – MATERIALS AND METHODS

2.1 Yeast Strains and Plasmids

All strains used in this study are isogenic to S288C (Table 2.1). Yeast culture and genetic manipulations were carried out using standard protocols (Smith and Burke 2014). Genomic deletions and epitope-tag integrations were verified by PCR analysis (Table 2.2 and Table 2.3). The strains carrying the histone H3 tail mutants were derived by plasmid shuffle from FY2162 (Duina and Winston 2003). The plasmid pGAL1prHHO1 was generated by cloning the *HHO1* open reading frame (ORF) into the BamHI and XhoI sites of pGAL1pr (Mumberg *et al.* 1994). The pHHT2prHHO1HA plasmid was created by, swapping the *GAL1* promoter from pGAL1prHHO1 with a fragment containing 535 bp upstream of the *HHT2* gene and adding a triple HA tag. All plasmids used in this study are listed in Table 2.4.

Table 2.1: Yeast strains used in this study

Yeast Strain	Mating Type	Genotype
Y7092	Mat α	*can1Δ::STE2pr-Sp-his5 lyp1Δ his3Δ1 leu2Δ0 met15Δ ura3Δ0*
YLH101	Mat a	*his3Δ200 leu2Δ1 lys2-128δ ura3-52 trp1Δ63*
YLH379	Mat a	*his3Δ200 leu2Δ1 lys2-128δ ura3-52 trp1Δ63 hho1::TRP*
YLH380	Mat a	*his3Δ200 leu2Δ1 lys2-128δ ura3-52 trp1Δ63 HHT2HA::HISMX6*
YLH945	Mat a	*his3Δ200 leu2Δ1 lys2-128δ ura3-52 trp1Δ63 hda1:KAN*
YLH948	Mat a	*his3Δ200 leu2Δ1 lys2-128δ ura3-52 trp1Δ63 rpd3::KAN*
YLH950	Mat a	*his3Δ200 leu2Δ1 lys2-128δ ura3-52 trp1Δ63 rco1::KAN*
YLH972	Mat a	*his3Δ200 leu2Δ1 lys2-128δ ura3-52 trp1Δ63 HISMX6-HAHHO1*
YLH224	Mat a	*his3Δ200 leu2Δ1 lys2-128δ ura3-52 trp1Δ63 (hht1-hhf1)::LEU2 (hht2-hhf2)::HIS3 Ty912Δ35::his4*

Table 2.2: Primers used to generate knock-out strains in this study

Primer	Sequence (5' to 3')
HDA1 F1	ATGGATTCTGTAATGGTTAAGAAAGAAGTACTGGA AAATCCGGATCCCCGGGTTAATTAA
HDA1 R1	TTTATTATTATTCAACTTTCATAAGGCATGAAGGT TGCCGGAATTCGAGCTCGTTTAAAC
RPD3 F1	CATACAAAACATTCGTGGCTACAACTCGATATCCGT GCAGCGGATCCCCGGGTTAATTAA
RPD3 R1	TCACATTATTTATATTCGTATATACTTCCAACTCTT TTTTGAATTCGAGCTCGTTTAAAC
RCO1 F1	ATAAAAGACACTTCCATTACCATCTGCTAATAATA ATACACGGATCCCCGGGTTAATTAA
RCO1 R1	TTCACGTTCCTGATTTATTCTTTATGTATGTACGCC GTTTGAATTCGAGCTCGTTTAAAC

Table 2.3: Primers used to verify knock-out strains in this study

Primer	Sequence (5' to 3')
HDA1 s-220	TCCCGCACCGTTTGGAAATC
HDA1 a+383	GAGGTTGCGGCTCTTACAG
RPD3 s-181	GGCTTTCGGGAAGCAAAGTG
RPD3 a+393	ATGCCCAATATTACGGCCCA
RCO1 s-173	CTCGCTGCAAGATCTGCCTC
RCO1 a+247	CCTTGGGTTCTTCTTCCGGG

Table 2.4: Plasmids used in this study

Plasmid	Description
p123	pRS416
p249	pGAL1.416
p964	pHHT2prHHO1HA.416
p658	pGAL1prHHO1.416
p311	pHHT2K9,14,18,23R
p696	pHHT2K9,14,18,23Q

2.2 Quantitative Immunoblot Analysis

Whole cell extracts (Kushnirov 2000) were loaded onto 15% polyacrylamide gels and run at 150 V at room temperature for 1 hour. Following separation, gels were equilibrated in equilibration buffer (62.5 mM Tris pH 6.8, 2.3% SDS) at room temperature for 30 min with shaking. Proteins were transferred to nitrocellulose membranes in transfer buffer (17 mM glycine, 0.15% ethanolamine, 0.2% methanol) at 100 V at room temperature for 1 hour. Nitrocellulose membranes were blocked with 2% BSA (HyClone™) for 1 hr at room temperature with shaking. Following blocking, membranes were incubated in primary

antibodies (Table 2.5) with PBS-T overnight at 4°C with shaking. Next, membranes were washed with PBS-T for 3 X 10 min at room temperature with shaking and incubated with secondary antibodies for 1 hr at room temperature with shaking, followed by fluorescence detection and quantification using the Licor Odyssey System.

Table 2.5: Antibodies used in this study

Antibody	Animal	Company	Catalogue Number
αH3	Rabbit	GeneScript	Raised against scH3 peptide (CKDILARRLRGERS)
αHho1	Rabbit	Abcam	ab71833
αHA	Mouse	Roche	11666606001
αHA	Rat	Roche	11867431001

2.3 Chromatin Immunoprecipitation-Quantitative PCR Analysis

Chromatin immunoprecipitation-quantitative PCR (ChIP-QPCR) analysis was performed as previously described (Martin *et al.* 2017). Cells were grown in 50 ml of synthetic drop-out media lacking uracil with galactose for 20 hr to an OD_{600} of ~0.8 and lysates were immunoprecipitated with 0.9 mg of α-Hho1 antibody (Table 2.5). QPCR was performed using the Applied Biosytems StepOnePlus Real-Time PCR System using the primers listed in Table 2.6.

Table 2.6: ChIP-QPCR primers used in this study

Primer	Sequence (5' to 3')
PMA1 a+85	CCTACGATGACGCTGCATC
PMA1 s+232	CCTCTGGAACTGGTCTAGC
SEC15 a+2230	GACCCATGAATTGTCTCGTCAAGG
SEC15 s+2082	GTAAGGCAAGACCCGGATATCTC
SEC15 a+370	GCACCATACCTTGGATGTTTGC
SEC15 s+230	GGACCCCGTAATTGATGAATTGG
LOS1 a+1395	CAGACTTGGGTCAATTACCACG
LOS1 a+2940	GTCGTCATTATCCAAGCAGGTCC
LOS1 a+230	CCATTTGGATTAGCGTTCACGC
LOS1 s+69	CAAGCCATCGAGCTGCTAAATG
PUT4 a+714	CACGCATAGAAAGATCGTGATCC
PUT4 s+546	CTGGTCACTAGGTACGTTGAC

2.4 Micrococcal Nuclease Digestion of Yeast Chromatin

Cells were grown in synthetic drop-out media lacking uracil with dextrose until stationary phase, before being washed two times in synthetic drop-out media lacking uracil with galactose. Cells were then diluted in –uracil galactose media to an OD_{600} of 0.2 and grown for 20 hr at 30°C. Following harvest, 25 ODs of cells were resuspended in 400 ml of 1 M sorbitol, 5 mM β-mercaptoethanol and 10 mg/ml zymolyase, and incubated at 37°C for 10 min. Spheroplasts were washed once in 1 M sorbitol and twice in spheroplast digestion buffer (SDB) (1 M sorbitol, 50 mM NaCl, 10 mM Tris pH 8, 5 mM MgCl2, 1 mM CaCl2, 1 mM β-mercaptoethanol, 0.5 mM spermidine, 0.075% NP40) before being resuspended in 450 ml of SDB. Samples were digested with varying concentrations of micrococcal nuclease (MNase) for 2 min and digestions were stopped by addition of EDTA and SDS to final

concentrations of 5 mM and 1%, respectively. Crosslinks were reversed by overnight incubation at 65°C and DNA was purified by digestion with proteinase K, phenol:chloroform:isoamyl extraction and ethanol precipitation. Samples were resuspended in 10 mM Tris pH 8, 1 mM EDTA and treated with RNase A prior to running on a 2% agarose gel. DNA was visualized using syto60 fluorescence detection with the Licor Odyssey System.

2.5 Synthetic Dosage Lethality Screen

The synthetic genetic array (SGA) starting strain Y7092 (MATα *can1Δ::STE2pr-Sp-his5 lyp1Δ his3Δ1 leu2Δ0 met15Δ ura3Δ0*) was transformed with pGAL1prHHO1. The resulting query strain was mated to the MATa deletion mutant array. SGA methodology, previously described for a plasmid-based synthetic dosage resistance screen (Chruscicki *et al.* 2010), was performed in triplicate with the following modifications: (1) medium lacking uracil was used to maintain the plasmid and (2) hits were scored against strains containing pGAL1prHHO1 grown on dextrose using the Balony program (Young and Loewen 2013). Hits were verified using PCR confirmation of the deletion strain, followed by transformation and dilution plating on appropriate media.

2.6 ChIP-Sequencing Analysis

ChIP-sequencing (ChIP-seq) was performed as previously described with a few alterations (Maltby *et al.* 2012b; a). Briefly, cells were grown in 1 liter of yeast, peptone, dextrose

media to mid-log phase and crosslinked with 1% formaldehyde for 15 min at 30°C. The cross-linking reaction was stopped with 125 mM glycine and cells were washed twice with cold PBS. Cells were resuspended in lysis buffer [50 mM HEPES-KOH (pH 7.5), 140 mM NaCl, 1mM EDTA, 1% Triton X-100, 0.1% sodium deoxycholate], flash frozen in liquid nitrogen and ground in a coffee grinder with dry ice for 10 X 3 min. Samples were thawed, normalized by protein content and sonicated (Diagenode Biorupter, high output for 30 X 30 sec on/off) to obtain an average DNA fragment length of 200–400 bp. The lysate was cleared at 10,000 rpm for 10 min and the supernatant was retained for the whole cell extract. Magnetic Protein-G Dynabeads were added and incubated with the whole cell extract for 1 hr and then removed. Antibodies were added (15.0 ml of the α-Hho1 antibody, Table 2.5) and incubated with the whole cell extract overnight. Magnetic Protein-G Dynabeads were added and incubated with the sample for 30 min. After reversal of crosslinking and DNA purification, the library construction protocol was performed as described (Maltby *et al.* 2012a)**.** Equimolar amounts of indexed, amplified libraries were pooled, adapter dimers were removed by gel purification and paired-end 100 nucleotide reads were generated using v3 sequencing reagents on the HiSeq2000 (SBS) platform. Reads were aligned to the Saccer3 genome using Bowtie2 (Langmead and Salzberg 2012) and plot2DO (https://github.com/rchereji/plot2DO**)** (Chereji *et al.* 2017)**,** deepTools (Ramírez *et al.* 2014; 2016) and the JavaGenomicsToolkit (http://palpant.us/java-genomics-toolkit/) were used for all subsequent analysis as indicated. Additional data used were sourced from https://www.ncbi.nlm.nih.gov/geo/ including GSE61888 (ChIP-seq of histone post-translational modifications in *S. cerevisiae*), GSE38384 (RNAPII ChIP-seq in *S.*

cerevisiae), GSE46134 (ChIP-seq of linker histones in mouse embryonic stem cells) and GSE29218 (ChIP-seq of H3K9ac, H3K27ac and RNAPII in mouse embryonic stem cells).

2.7 Data Availability

The ChIP-seq data generated for this study have been deposited in the Gene Expression Omnibus (GEO) database (www.ncbi.nlm.nih.gov/geo/), GEO accession no. GSE100591.

CHAPTER 3 – RESULTS

3.1 Refining linker histone stoichiometry in *S. cerevisiae*

Most eukaryotic chromatin contains approximately one molecule of linker histone for every nucleosome. In *S. cerevisiae*, linker histone stoichiometry is greatly reduced, but attempts to quantify the ratio of linker histone to nucleosomes have led to conflicting results. Previous studies made use of carboxyl-terminal epitope tags to quantify Hho1 levels but, surprisingly, we found that addition of a carboxyl-terminal HA tag to the endogenous *HHO1* gene reduced Hho1 abundance approximately five-fold (Figure 3.1A and B). One explanation for this effect is the native *HHO1* 3'-UTR, which is replaced when carboxyl-terminal epitope tagging, is required for mRNA stability or protein translation. To circumvent this problem, we sought to quantify the abundance of Hho1 expressed from an unaltered *HHO1* locus relative to a core histone. To this end, we generated a yeast strain expressing two copies of *HHO1* (Figure 3.2A). The first copy was the endogenous, chromosomal *HHO1* locus, which was unaltered (shown in yellow). The second copy was the *HHO1* ORF (yellow) fused to the histone H3 promoter (*HHT2pr*, shown in red) with a carboxyl-terminal HA tag (blue) on a low-copy plasmid. The yeast strain also included an identical HA tag on one (*HHT2*) of the two copies of the histone H3 gene. By immunoblotting whole cell extracts from this strain for Hho1, HA and H3, we could directly compare signals generated with the Hho1 and H3 antibodies, using the identical HA tags on Hho1 and H3 (Figure 3.2B). Using this approach, with three biological replicates, we

calculated the linker histone stoichiometry in yeast to be one molecule of linker histone generated from the endogenous *HHO1* locus for every 18.9 $\pm$ 1.0 nucleosomes.

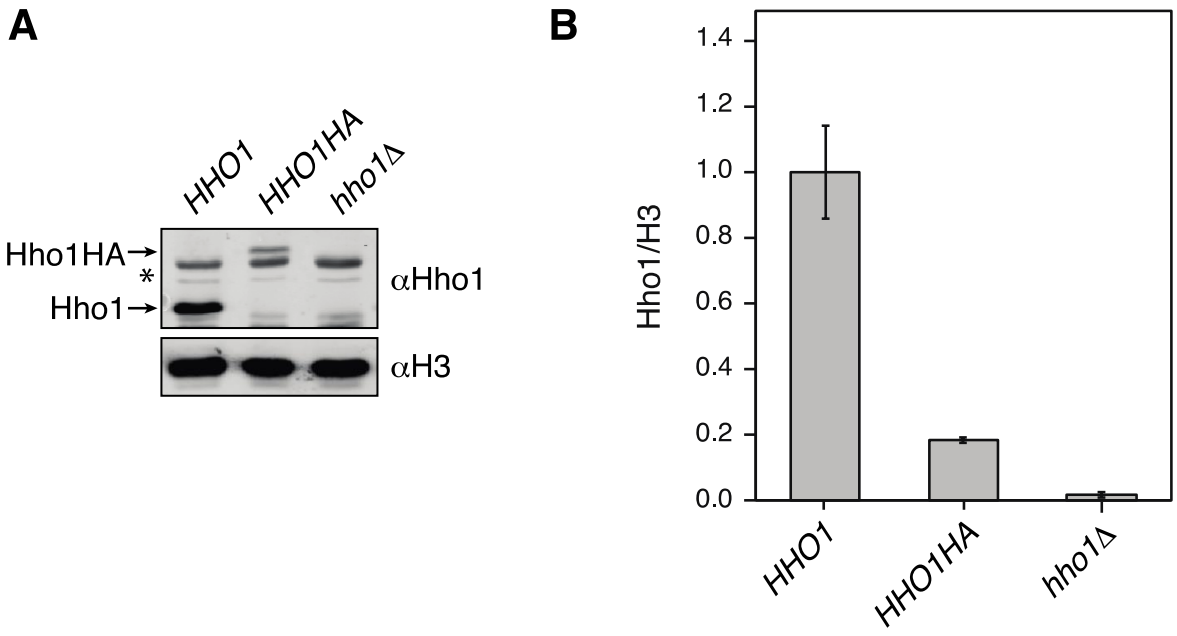

Figure 3.1: Quantifying endogenous Hho1 levels in *S. cerevisiae*
(A) Immunoblot analysis of Hho1 levels in whole cell extracts from wild type cells (*HHO1)* and cells with an HA-tag integrated at the carboxyl terminus of the endogenous *HHO1* gene (*HHO1HA*). Histone H3 was used as a loading control. A band cross-reacting with the αHho1 antibody is indicated with an asterisk. (B) Quantification of Hho1 levels determined from immunoblot of Hho1 normalized to histone H3. Bars indicate the standard error of the mean from three biological replicates.

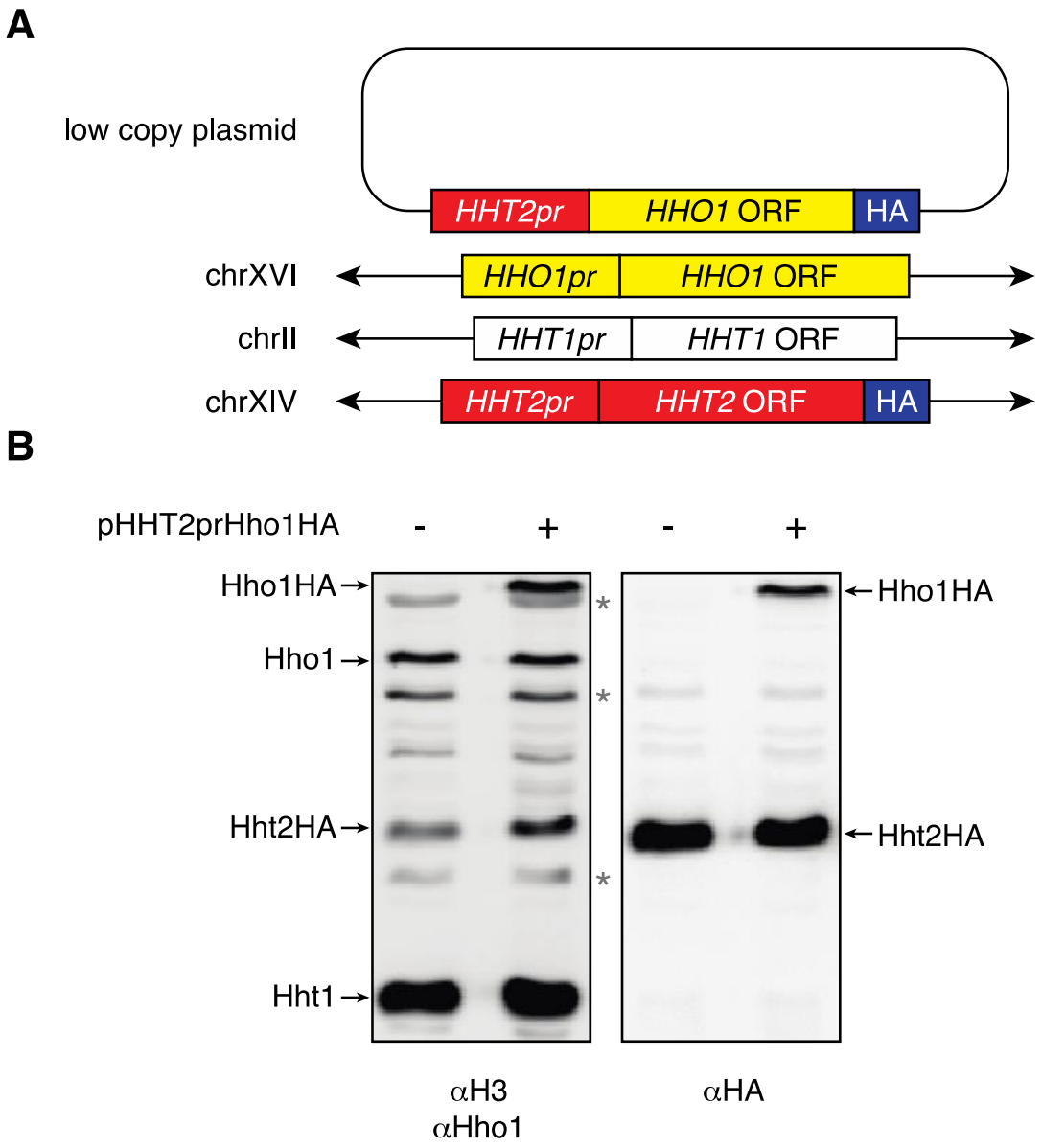

Figure 3.2: Refining linker histone stoichiometry in *S. cerevisiae*

(A) Schematic representation of the genes encoding histones Hho1 and H3 in an engineered strain of *S. cerevisiae*. Elements from the *HHO1* locus are shown in yellow, the *HHT1* (Histone H Three 1) locus are shown in white and *HHT2* (Histone H Three 2) locus are shown in red. The position of triple HA tags on Hho1 and Hht2 are shown in blue. pr, promoter. (B) Representative immunoblot of whole cell extracts from the strain described in A (+) as well as an isogenic strain lacking the pHHT2prHHO1 plasmid (2). Quantification of Hho1HA with αHA and αHho1 antibodies and H3 with αHA and αH3 antibodies facilitated determination of the relative ratio

of Hho1 to histone H3. Bands cross-reacting with the αHho1 antibody are indicated with asterisks.

3.2 Increased linker histone stoichiometry is toxic in *S. cerevisiae*

Linker histones are thought to negatively regulate transcription and thus the reduced linker histone stoichiometry in *S. cerevisiae* is consistent with the gene-dense nature of the yeast genome. To determine the impact of increased linker histone dosage on growth and chromatin structure of *S. cerevisiae*, we fused the *HHO1* ORF to a *GAL1* promoter (*GAL1pr*) on a low-copy vector and transformed this plasmid into wild-type yeast. Expression of Hho1 from *GAL1pr* resulted in a severe growth defect (Figure 3.3A), despite increasing total Hho1 abundance only threefold relative to yeast with vector alone (Figure 3.3A, B and C).

To confirm that excess Hho1 is incorporated into chromatin, we performed chromatin immunoprecipitation at multiple loci, including the 5' end of a highly expressed gene (*PMA1*), the 5' and 3' ends of two moderately expressed genes (*LOS1* and *SEC15*) and the middle of *PUT4*, an inactive gene. These results, shown in Figure 3.3D, demonstrate that *HHO1* overexpression resulted in statistically significant increases (*p*-value for student's *t*-test, < 0.05) in Hho1 occupancy at all loci tested, with the exception of *PUT4*. Importantly, in no case was the increase in Hho1 occupancy proportional to the over threefold increase in total Hho1 abundance observed in Figure 3.3B and C, suggesting that in yeast, linker histone binding is not strictly dictated by Hho1 levels. Interestingly, the greatest increases

in Hho1 binding upon *HHO1* overexpression were observed on the 5' ends of genes. Previous work has shown that Hho1 is enriched in regions with increased nucleosome spacing (Ocampo *et al.* 2016). To determine whether the differential incorporation of excess Hho1 at 5' relative to 3' genic regions was due to increased nucleosome spacing, we calculated the average spacing of nucleosomes relative to all annotated TSSs in yeast (Weiner *et al.* 2015). Figure 3.3E shows that average nucleosome spacing between the +1 and +2, +2 and +3, and +3 and +4 nucleosomes is 167, 165, and 164 bp, respectively. In contrast, average nucleosome spacing between the +4 and +5, and +5 and +6 nucleosomes is 161 bp, suggesting that these regions are refractory toward Hho1 binding because they lack sufficient linker DNA.

To determine whether *HHO1* overexpression was associated with major changes in chromatin structure, we analyzed the effect of increased Hho1 on the sensitivity of yeast chromatin to micrococcal nuclease (MNase). Figure 3.3, F and G show that increased Hho1 levels had little effect on the length of fragments generated by MNase digestion. However, *HHO1* overexpression consistently resulted in loss of fragments larger than four nucleosomes and the generation of a high molecular weight, MNase-resistant DNA band (highlighted with an asterisk in Figure 3.3F), which may suggest that increased levels of Hho1 promotes the formation of nuclease-resistant domains at the expense of longer MNase-sensitive, nucleosome arrays. Collectively, these results demonstrate that overexpression of Hho1 results in modest increases in Hho1 occupancy at the 5' regions of genes, localized changes in chromatin structure and impaired cell growth.

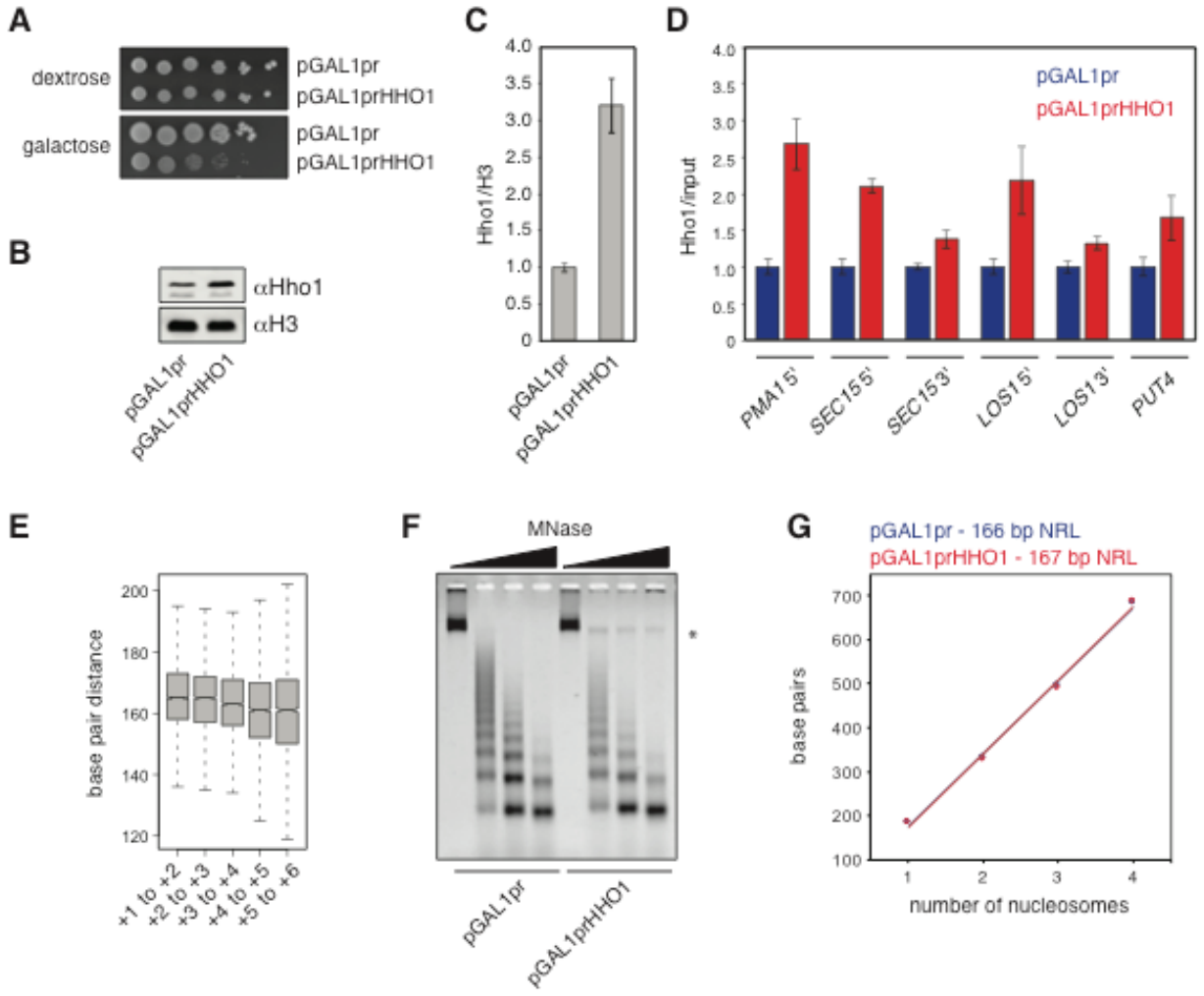

Figure 3.3: Increased linker histone stoichiometry is toxic in *S. cerevisiae*

(A) Ten-fold serial dilutions of wild-type yeast containing vector alone (pGAL1pr) or expressing *HHO1* from a *GAL1* promoter (pGAL1prHHO1) were plated on uracil drop-out media with dextrose or galactose and grown at 30°C for 3 days. (B) Representative immunoblot for Hho1 levels in extracts from cells with vector alone (pGAL1pr) or expressing *HHO1* from a *GAL1* promoter (pGAL1prHHO1) grown for 20 hr in uracil drop-out media with galactose. (C) Quantification of Hho1 levels determined from immunoblot of Hho1 in three biological replicates. Error bars indicate the SE of the mean. (D) ChIP-QPCR for galactose-induced Hho1 at the indicated loci. Cells containing vector alone were set to 1. Error bars indicate SE of the mean of six biological replicates. (E) Box plot of base pair distance between nucleosome positions (Weiner *et al.* 2012) relative to the transcriptional start site. Notches indicate the 95%

confidence interval for the median. (F) Chromatin from cells containing vector alone (pGAL1pr) or expressing *HHO1* from a *GAL1* promoter (pGAL1prHHO1) grown for 20 hr in uracil drop-out media with galactose was digested with increasing concentrations of MNase. The DNA was purified and resolved on an agarose gel. (G) Plot of DNA fragment sizes (from F) vs. the number of nucleosomes with cells containing vector alone (blue) or expressing *HHO1* from a *GAL1* promoter (red). The indicated nucleosome repeat lengths were determined from the slope of the lines.

The specific incorporation of excess Hho1 at the 5' regions of genes was surprising, considering that previously published work suggests that Hho1 fails to cross-link to the 5' linker DNA of +1 nucleosomes (Rhee *et al.* 2014). This inconsistency may suggest that, when expressed from its endogenous promoter, Hho1 binding is under some form of regulation. To identify proteins or genetic pathways involved in regulating the interaction of Hho1 with chromatin, we used SGA technology to overexpress Hho1 in the ~4700 non-essential yeast deletion mutants. A major class of genes identified in the screen was those that regulate core histone gene dosage (Figure 3.4) (Kurat *et al.* 2014). Interestingly, decreased growth due to *HHO1* overexpression was observed in mutants predicted to have both decreased and increased histone levels (chi-squared test, $P = 0.00263$ for a random distribution). The sensitivity of cells with increased core histone levels to Hho1 overexpression was not surprising, as the combination likely interferes with processes that use DNA as a template. In contrast, the enhanced Hho1 toxicity of cells with reduced core histone levels may be due to increased nucleosome spacing, which creates additional binding sites for Hho1, interfering with DNA access. Indeed, *spt10Δ*, one of the most sensitive strains to *HHO1* overexpression, has been shown to exhibit increased nucleosomes spacing (van Bakel *et al.* 2013).

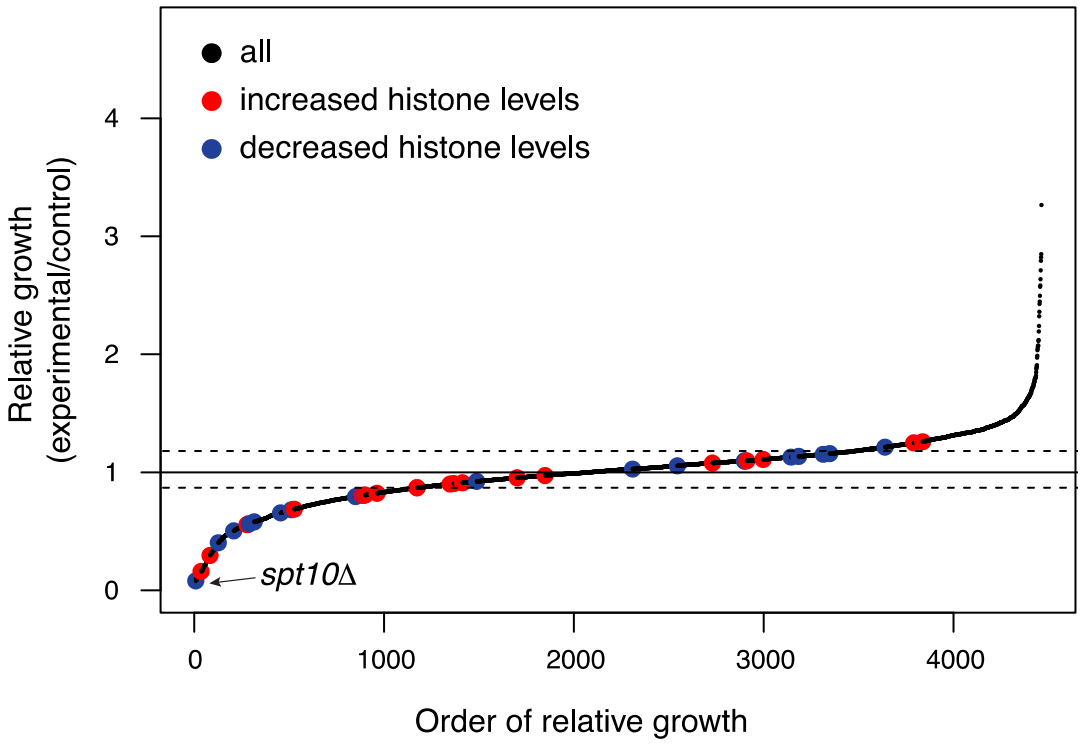

Figure 3.4: Altered histone levels exacerbate toxicity due to increased linker histone stoichiometry in *S. cerevisiae*

Relative growth of ~4700 non-essential deletion strains expressing Hho1 from a *GAL1* promoter. Mutants that are predicted to have decreased and increased histone levels are shown in blue and red, respectively (Kurat et al. 2014). Values above 1.0 reflect improved growth and values below 1.0 reflect decreased growth. Dashed lines denote default thresholds for rescues and lethality.

3.3 Histone acetylation negatively regulates linker histone binding in *S. cerevisiae*

A second class of genes identified in our synthetic dosage screen was those encoding HDACs (Figure 3.5A). However, contrary to mutants with altered histone dosage, mutation of HDACs rescued Hho1 toxicity. To verify that loss of an HDAC could rescue growth of cells with excess Hho1, we created an *hda1Δ* mutant in our laboratory strain background and confirmed resistance to Hho1 overexpression by dilution plating (Figure 3.5B). We also confirmed that rescue of growth in an *hda1Δ* mutant was not due to a *GAL1* transcription defect by quantitative immunoblot (Figure 3.5C). To verify that the impact of HDAC loss is due to loss of deacetylation of core histones, we mutated acetylation sites in the tail of histone H3 to arginine and glutamine to mimic unacetylated and acetylated lysine residues, respectively. In strains overexpressing Hho1, glutamine substitutions in the H3 tail conferred a growth advantage (Figure 3.5D), which was not due to altered Hho1 levels (Figure 3.5E). Collectively, these results suggest that histone acetylation negatively regulates the binding of Hho1 to chromatin.

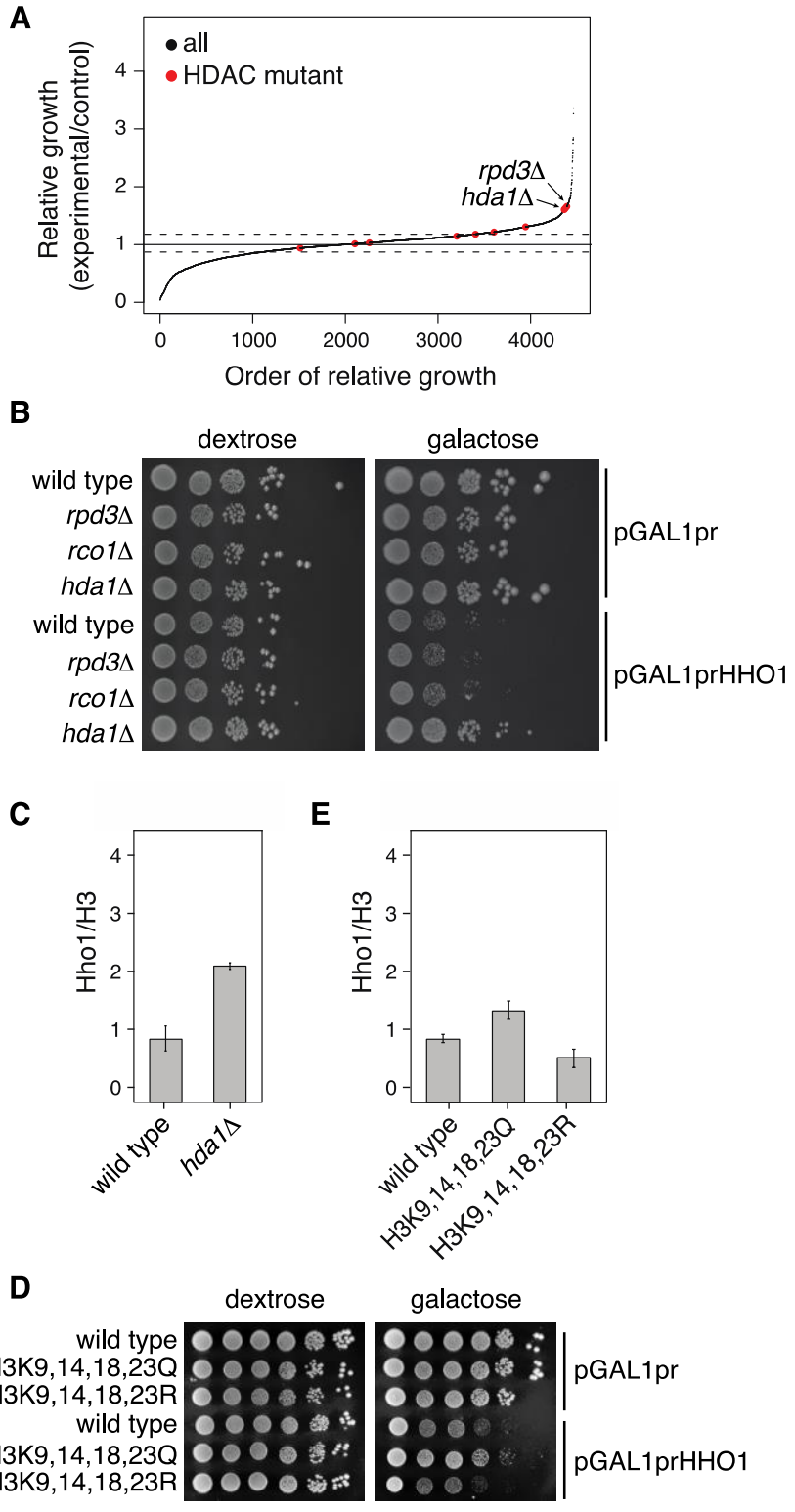
A
all
HDAC mutant
Relative growth (experimental/control)
rpd3Δ
hda1Δ
Order of relative growth
B
dextrose
galactose
wild type
rpd3Δ
rco1Δ
hda1Δ
wild type
rpd3Δ
rco1Δ
hda1Δ
pGAL1pr
pGAL1prHHO1
C
Hho1/H3
wild type
hda1Δ
E
Hho1/H3
wild type
H3K9,14,18,23Q
H3K9,14,18,23R
D
dextrose
galactose
wild type
H3K9,14,18,23Q
H3K9,14,18,23R
wild type
H3K9,14,18,23Q
H3K9,14,18,23R
pGAL1pr
pGAL1prHHO1

Figure 3.5: Histone acetylation negatively regulates linker histone binding in *S. cerevisiae*
Relative growth of ~4700 non-essential deletion strains expressing Hho1 from a *GAL1* promoter. Mutants with gene deletions of *RPD3, HDA1, HOS1, HOS2, HOS3, HOS4, HST1, HST2, HST3* and *HST4* are shown in red. (B and D) Ten-fold serial dilutions of the indicated strains carrying either vector alone (pGAL1pr) or a plasmid expressing *HHO1* from a *GAL1* promoter (pGAL1prHHO1) were grown on uracil drop-out media, with either dextrose or galactose as indicated, at 30^{o}C for 4 days. (C and E) Immunoblot quantification of Hho1 levels in the indicated strains expressing *HHO1* from a *GAL1* promoter after growth for 20 hr in uracil drop-out media with galactose. Error bars indicate the SE of the mean from three biological replicates.

To further investigate the role of histone acetylation in regulating Hho1 binding, we performed ChIP-seq analysis of Hho1 expressed from its native promoter. To visualize the data generated, we used 2D occupancy plots, which simultaneously display DNA sequencing data as: (1) the relative sequence read abundance (heatmap), (2) sequence fragment length (y-axis) and (3) position of sequence reads relative to the dyad of the +1 nucleosome (x-axis with the white dashed line indicating the +1 dyad) (Chereji *et al.* 2017). This analysis, presented in Figure 3.6A, shows that the input DNA used for ChIP was slightly enriched in sequences –400 to +100 bp relative to the +1 nucleosome (left panel) and contained mononucleosome-sized DNA fragments, with the peak of distribution at ~165 bp (right panel). In contrast, Hho1 antibodies immunoprecipitated primarily larger fragments with a peak of distribution of ~270 bp (right panel). Interestingly, smaller fragments were present in the Hho1 ChIP, but few small fragments overlapped the +1 nucleosome (middle panel), despite being present in the input (left panel). In contrast, reads overlapping the +1 nucleosome were precipitated with Hho1 if they were longer and also overlapped the +2 nucleosome. Collectively, these data argue that the +1 nucleosome

is depleted in Hho1 such that these nucleosomes can only be precipitated with Hho1 antibodies if linked to a +2 nucleosome. This is consistent with previously published work demonstrating that Hho1 fails to cross-link to the 5' linker of the +1 nucleosome (Rhee *et al.* 2014).

Depletion of Hho1 over the +1 nucleosomes is consistent with the fact that these nucleosomes tend to be highly acetylated. To determine if histone acetylation and Hho1 inversely correlate genome-wide, we quantified the levels of Hho1 and multiple histone post-translational modifications (Weiner *et al.* 2015) over the 67,523 annotated yeast nucleosomes (Brogaard *et al.* 2012) and generated a pairwise Spearman correlation matrix with hierarchical clustering. Figure 3.6B shows that Hho1 occupancy clustered with histone H4R3 mono-methylation and H2AS129 phosphorylation. Little is known about the function of H4R3 methylation in yeast, but H2AS129p is enriched at repressed protein-coding genes (Szilard *et al.* 2010), consistent with a role of Hho1 in negatively regulating transcription. In contrast, except for H4K16ac, all histone acetylation marks in yeast clustered away from Hho1 occupancy with inverse correlation coefficients consistent with the negative regulation of linker histone binding by histone acetylation.

An explanation for the inverse correlation between acetylation and linker histone occupancy observed in Figure 3.6B is that transcription, which is linked to acetylation, disrupts the interaction of Hho1 with chromatin. Indeed, data supporting this possibility have been published (Schafer *et al.* 2008). To discount a role of transcription in regulating Hho1 binding, we took advantage of the fact that the association between acetylation and

transcription is not absolute. For example, while RNAPII traverses the entirety of a gene, histone acetylation is primarily limited to the 5' end of the transcribed unit. Thus, pools of nucleosomes can be identified that share similar levels of RNAPII but have different amounts of histone acetylation. To determine whether the inverse correlation between Hho1 and histone acetylation is due to the presence of RNAPII, we divided yeast nucleosomes into quartile bins based on RNAPII occupancy as determined in Hobson *et al.* (2012). We further divided each of the resulting bins based on histone acetylation and identified nucleosomes in each bin with high (top quartile, blue) and low (bottom quartile, red) levels of H3K23ac or other acetylation marks (Weiner *et al.* 2015). Figure 3.6, C and D show the amounts of RNAPII and H3K23ac in the eight resulting bins, respectively. We then calculated Hho1 occupancy for each bin and plotted it as a box plot (Figure 3.6E for H3K23ac and Figure 3.7 for other acetylation sites). The results show that nucleosomes with increased H3K23ac had reduced Hho1 occupancy when levels of RNAPII were normalized, indicating that differing RNAPII levels were not responsible for altered Hho1 occupancy. Similar trends were observed when analyzing other acetylation marks (Figure 3.7). Additionally, comparable results were obtained when analyzing linker histone H1.2, H1.3 and H1o occupancy (Cao *et al.* 2013) in mouse embryonic stem cells relative to H3K9ac (Figure 3.8, A–E) and H3K27ac (Figure 3.8F). Collectively, these results suggest that acetylated chromatin is refractory to linker histone binding in *S. cerevisiae* and other organisms.

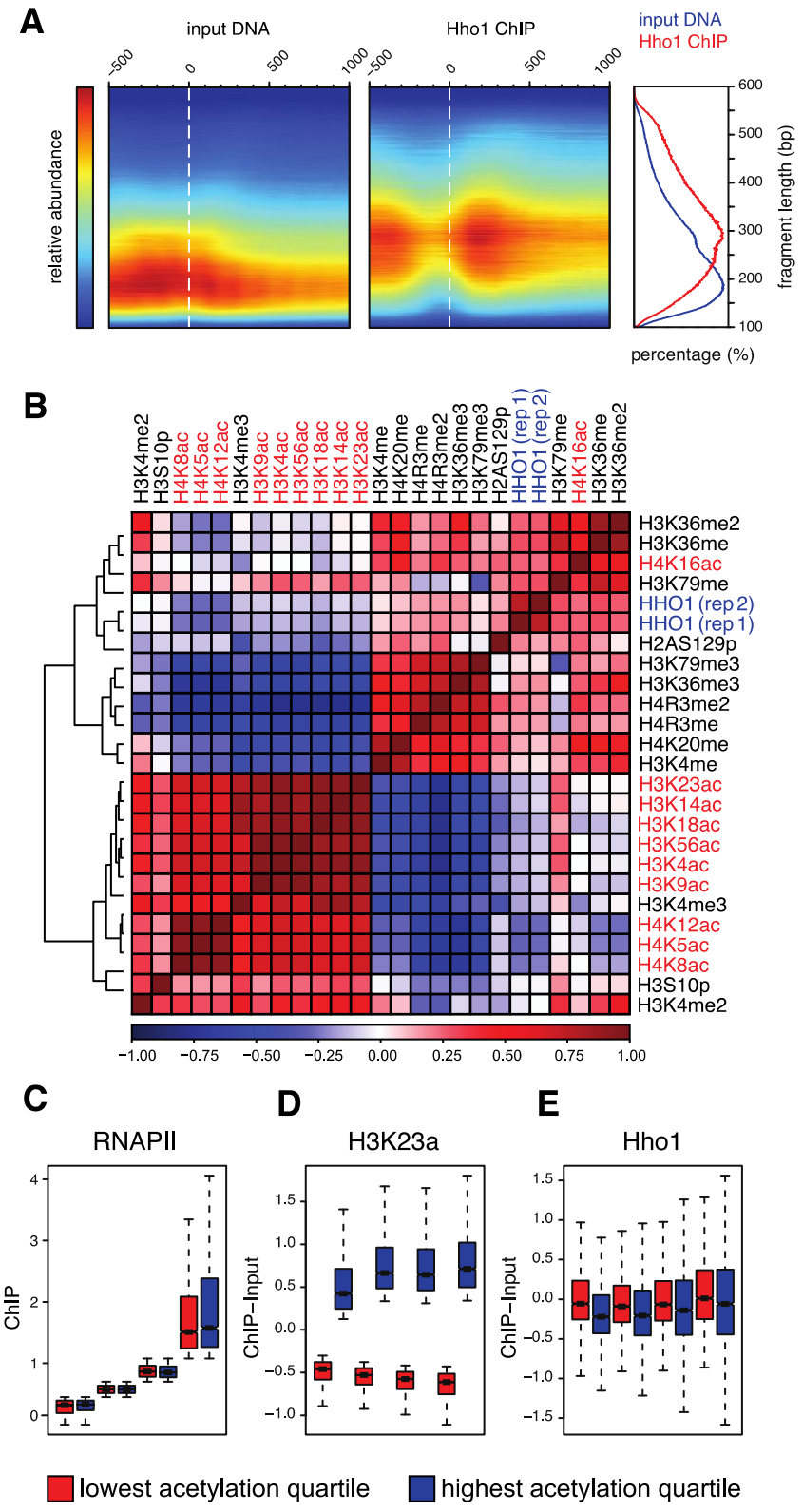
A
input DNA
Hho1 ChIP
input DNA
Hho1 ChIP
relative abundance
fragment length (bp)
percentage (%)
B
H3K36me2
H3K36me
H4K16ac
H3K79me
HHO1 (rep 2)
HHO1 (rep 1)
H2AS129p
H3K79me3
H3K36me3
H4R3me2
H4R3me
H4K20me
H3K4me
H3K23ac
H3K14ac
H3K18ac
H3K56ac
H3K4ac
H3K9ac
H3K4me3
H4K12ac
H4K5ac
H4K8ac
H3S10p
H3K4me2
C
RNAPII
ChIP
D
H3K23a
ChIP−Input
E
Hho1
ChIP−Input
lowest acetylation quartile
highest acetylation quartile

Figure 3.6: Histone acetylation negatively correlates with linker histone binding in *S. cerevisiae*

(A, left and middle) Two-dimensional occupancy plots of relative sequence fragment abundance, sequence fragment length and sequence fragment position from input DNA and Hho1 ChIP, relative to the dyad axis of the +1 nucleosomes of 5770 annotated genes in *S. cerevisiae*. Plot was generated using plot2DO (Chereji *et al.* 2017) run with standard settings. The relative sequence read abundance is indicated as a heatmap, the sequence fragment length is plotted on the y-axis and the position of sequence reads relative to the +1 nucleosome is plotted on the x-axis. (Right) Plot of sequence fragment lengths from input DNA and Hho1 ChIP-seq of wild-type yeast. (B) Clustered heatmap produced by the deepTools plotCorrelation module (Ramírez *et al.* 2014; 2016). Shown here are the Spearman correlation coefficients of Hho1 occupancy (blue text) at all uniquely mapping yeast nucleosomes (Brogaard *et al.* 2012) with histone post-translational modifications (Weiner et al. 2015), including histone acetylation (red text). All data sets were normalized to respective inputs using the deepTools bigwigCompare tool (C–E). All uniquely mapping yeast nucleosomes (Brogaard *et al.* 2012) were binned into quartiles based on RNAPII occupancy (C) and the top and bottom quartiles of H3K23ac (Weiner *et al.* 2015) (D). Hho1 occupancy was then plotted for each bin (E). Notches indicate the 95% confidence interval for the median.

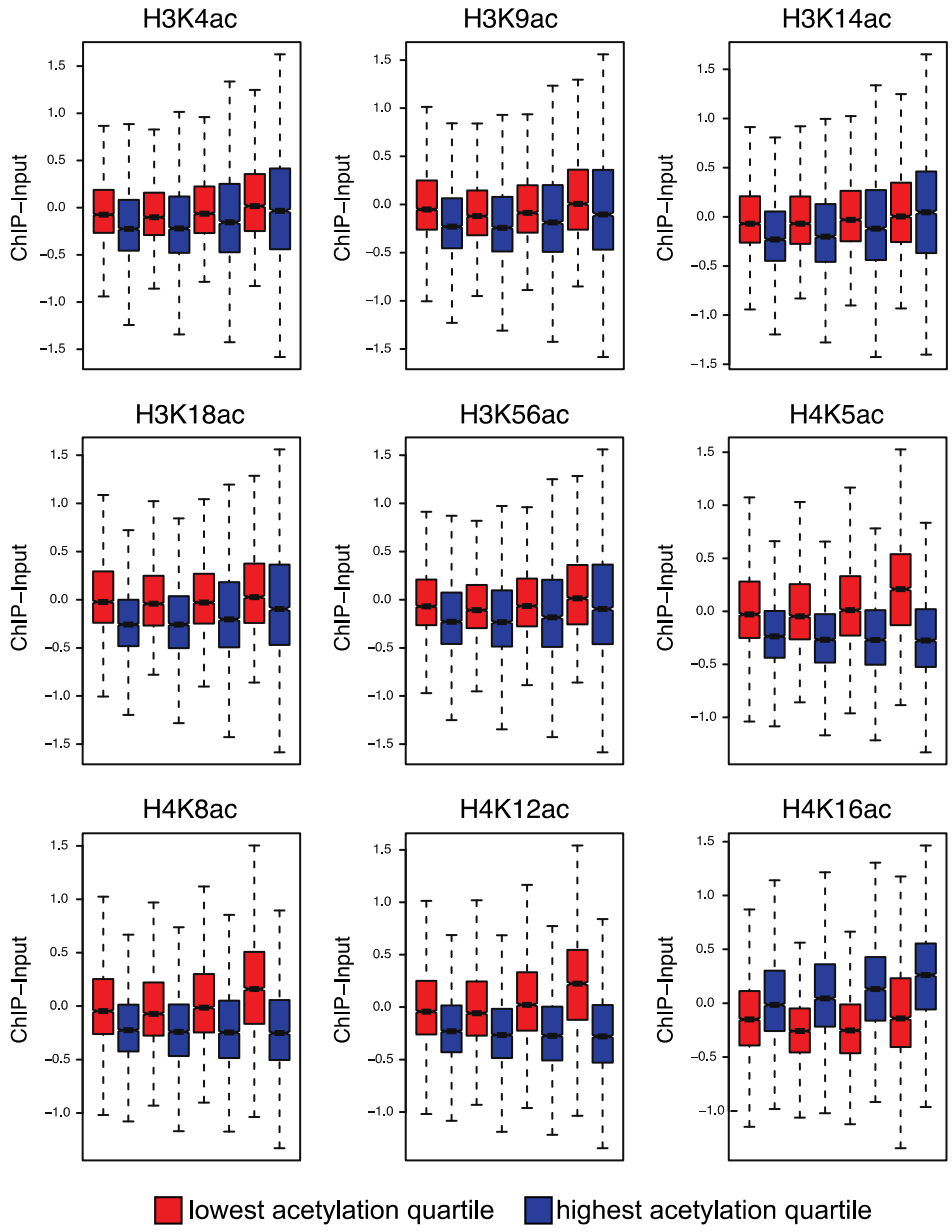

Figure 3.7: Histone acetylation negatively correlates with linker histone binding in *S. cerevisiae*

All uniquely mapping yeast nucleosomes (Brogaard et al. 2012) were binned into quartiles based on RNAPII occupancy (Figure 3.6C) and the top and bottom quartiles of the indicated histone acetylation marks (Weiner et al. 2015) were calculated using the Java Genomics Toolkit ngs.IntervalStats tool. Hho1 occupancy was then plotted for each bin. Notches indicate the 95% confidence interval for the median.

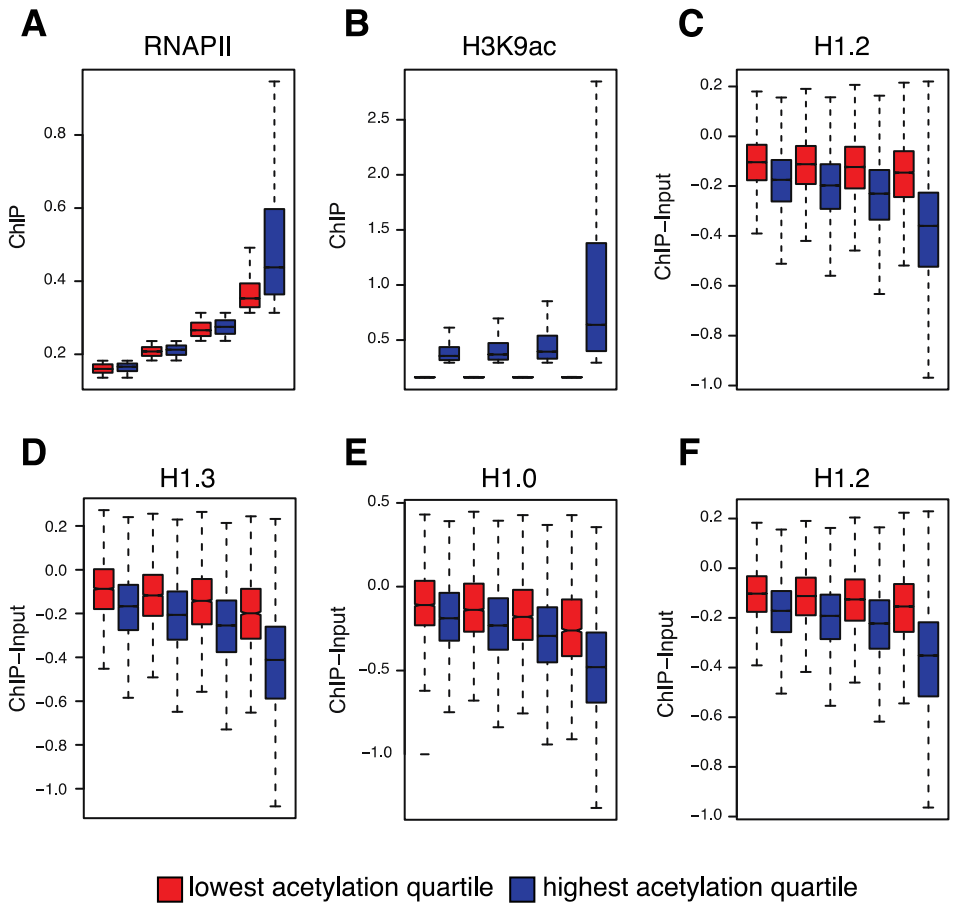

Figure 3.8: Histone acetylation negatively correlates with linker histone binding in mouse embryonic stem cells

The mouse genome was divided into 1000 bp windows, stepping 500 bp. Windows were divided into four quartiles based on RNAPII (GSM723019) occupancy (A) and the top and bottom quartiles for H3K9ac (GSM1000127) occupancy (B) as determined using the Java Genomics Toolkit ngs.IntervalStats tool. H1.2, H1.3 and H1o occupancies (Cao *et al.* 2013) were then plotted for each bin (C–E, respectively). Notches indicate the 95% confidence interval for the median. (F) Identical analysis as in C, but windows were binned based on H3K27ac (GSM1000099) instead of H3K9ac.

CHAPTER 4 – DISCUSSION

Refining linker histone stoichiometry

In this study, we investigated the regulation of linker histone binding in the yeast, *S. cerevisiae.* A major factor thought to regulate linker histone levels in chromatin is the abundance of linker histone in the cell. While vertebrate cells contain approximately one linker histone for every nucleosome, *S. cerevisiae* exhibits reduced linker histone levels; albeit the reported stoichiometry relative to nucleosomes varies depending on the study (Woodcock et al. 2006). Using a novel approach, we determined that yeast have one molecule of Hho1 for every ~19 nucleosomes. Previous work using various approaches have estimated the stoichiometry of Hho1 to nucleosomes to be 1:4, 1:10, 1:26 and 1:37 (Freidkin and Katcoff 2001; Downs et al. 2003; Ghaemmaghami et al. 2003; Kulak et al. 2014). Interestingly, the 1:26 ratio, which is the closest to our result, is the only previous study to quantify levels of un-tagged Hho1 (Kulak et al. 2014). Regardless of the exact ratio, all studies agree that Hho1 levels are well below that of nucleosomes and because linker histones bind and compact chromatin cooperatively (Routh et al. 2008), this may be important to prevent formation of higher-order chromatin structures on the gene-rich yeast genome.

Increased linker histone expression is toxic in yeast

Consistent with the importance of sub-stoichiometric linker histone levels in *S. cerevisiae*, increased expression resulted in a severe growth defect. Interestingly, this defect was

accompanied by only modest increases in linker histone levels at most loci tested. This result was initially surprising since in fibroblasts, overexpressed linker histones can bind chromatin, increasing the overall nucleosome repeat length (Gunjan *et al.* 1999). While we cannot exclude the fact that some of the overexpressed Hho1 is cytoplasmic and thus not available for chromatin binding, multiple lines of evidence support the hypothesis that short linker DNA in yeast chromatin excludes Hho1. First, previous work shows that Hho1 is enriched in regions with increased spacing between nucleosomes (Ocampo *et al.* 2016), suggesting that linker DNA availability as opposed to linker histone abundance, dictates Hho1 binding. Second, in stationary phase, genic nucleosomes increase their spacing (Zhang *et al.* 2011), which coincides with increased linker histone binding to chromatin (Schafer *et al.* 2008). Finally, chromatin reconstituted on DNA that positions nucleosomes with short linkers is resistant to linker histone binding and compaction (Routh *et al.* 2008). Collectively, these data suggest that histone stoichiometry does not dictate linker histone binding in yeast. Instead, overexpressed Hho1 likely localizes to limited regions with longer linker DNA, such as the 5' ends of genes, where it interferes with the early stages of transcription.

Histone acetylation negatively regulates linker histone binding

The preference of Hho1 for binding regions with longer linker DNA, makes the +1 nucleosome, which is adjacent to a nucleosome free region (NFR), a seemingly ideal ligand for binding by this linker histone. However, our data and that of others, show Hho1 depletion from the +1 nucleosome. The molecular basis for this observation was revealed

in this study using both genetic and genome-wide approaches, demonstrating that histone tail acetylation negatively regulates Hho1 binding. Since the 5' ends of transcribed genes are highly acetylated, these regions may be largely refractory to Hho1 binding. The ability of histone acetylation to hamper the binding of Hho1 is not surprising, as others have observed increased linker histone mobility in cells treated with HDAC inhibitors (Raghuram *et al.* 2010). Together our data support a model in which histone acetylation, not histone stoichiometry, plays a dominant role in regulating linker histone binding in *S. cerevisiae*. Moreover, our results shed light on the puzzling finding that despite their role in compacting chromatin, depletion of linker histones does not result in global upregulation of gene expression (Shen and Gorovsky 1996; Freidkin and Katcoff 2001; Fan *et al.* 2005a). Since acetylation likely excludes linker histones from regions of transcriptional activity, their depletion has little impact on steady-state transcription.

Does the GAL1 promoter induce the expected amount of Hho1 expression?

It is possible that a feedback mechanism exists in yeast to degrade excess free Hho1 in the cell. If this is the case, we would expect reduced Hho1 expression compared to other proteins expressed from the same *GAL1* promoter. However, deletion of *HDA1* which is expected to displace Hho1, does not result in reduced Hho1 levels in the cell. To explore this further, future experiments could upregulate Hho1 expression further using one or more high-copy plasmids to reach comparable levels of linker histones compared to nucleosomes. If no feedback mechanism exists in yeast to degrade free linker histones, we would expect higher Hho1 levels to result in exacerbated cellular toxicity.

Why is HHO1 overexpression toxic?

Clearly, increased linker histone levels are toxic in *S. cerevisiae*. One possible explanation could be that increased Hho1 binding over the 5' end of genes could inhibit RNAPII promoter escape or early elongation, resulting in transcription inhibition. Indeed RNAPII has been shown to accumulate at the 5' ends of genes (Churchman and Weissman 2011). To test this, native elongation transcript-sequencing (NET-seq) could be performed in cells overexpressing Hho1. Alternatively, toxicity could be due to ectopic Hho1 expression outside of S phase of the cell cycle. Hho1 along with the core histones are primarily expressed during S phase, and increased core histone levels results in compromised cellular fitness (Spellman *et al.* 1998; Kurat *et al.* 2014). This could be tested by expressing Hho1 from its endogenous promoter from one or more high-copy plasmids, ensuring overexpression occurs primarily during S phase. If ectopic expression of Hho1 is mediating toxicity, we would expect to see improved fitness compared to cells expressing a similar amount of Hho1 from the *GAL1* promoter.

Significance

This work supports a model in which core histone acetylation, which is a consequence of transcription, reinforces active transcription. Additionally, this adds to our understanding of how core histone acetylation promotes transcription in yeast and other organisms by regulating the binding of linker histones at transcribed genes. Moreover, if histone PTMs are heritable markers of gene expression states, this work provides a mechanism for the

epigenetic inheritance of linker histone levels and their associated transcriptional states via histone acetylation.

REFERENCES

Ali T., Thomas J. O., 2004 Distinct Properties of the Two Putative "Globular Domains" of the Yeast Linker Histone, Hho1p. Journal of Molecular Biology **337**: 1123–1135.

Ali T., Coles P., Stevens T. J., Stott K., Thomas J. O., 2004a Two Homologous Domains of Similar Structure but Different Stability in the Yeast Linker Histone, Hho1p. Journal of Molecular Biology **338**: 139–148.

Ali T., Coles P., Stevens T. J., Stott K., Thomas J. O., 2004b Two Homologous Domains of Similar Structure but Different Stability in the Yeast Linker Histone, Hho1p. Journal of Molecular Biology **338**: 139–148.

Allahverdi A., Yang R., Korolev N., Fan Y., Davey C. A., Liu C.-F., Nordenskiöld L., 2011 The effects of histone H4 tail acetylations on cation-induced chromatin folding and self-association. Nucleic Acids Research **39**: 1680–1691.

Allan J., Hartman P. G., Crane-Robinson C., Aviles F. X., 1980 The structure of histone H1 and its location in chromatin. Nature **288**: 675–679.

Allan J., Mitchell T., Harborne N., Bohm L., Crane-Robinson C., 1986 Roles of H1 domains in determining higher order chromatin structure and H1 location. Journal of Molecular Biology **187**: 591–601.

Allfrey V. G., Faulkner R., Mirsky A. E., 1964 Acetylation and methylation and their possible role in the regulaton of RNA synthesis. Proceedings of the National Academy of Sciences **51**: 786–794.

Arents G., Moudrianakis E. N., 1993 Topography of the histone octamer surface: repeating structural motifs utilized in the docking of nucleosomal DNA. Proceedings of the National Academy of Sciences **90**: 10489–10493.

Arents G., Moudrianakis E. N., 1995 The histone fold: a ubiquitous architectural motif utilized in DNA compaction and protein dimerization. Proceedings of the National Academy of Sciences **92**: 11170–11174.

Arents G., Burlingame R. W., Wang B. C., Love W. E., Moudrianakis E. N., 1991 The nucleosomal core histone octamer at 3.1 A resolution: a tripartite protein assembly and a left-handed superhelix. Proceedings of the National Academy of Sciences **88**: 10148–10152.

Ausió J., Van Holde K. E., 1986 Histone hyperacetylation: its effects on nucleosome conformation and stability. Biochemistry **25**: 1421–1428.

Bannister A. J., Kouzarides T., 2011 Regulation of chromatin by histone modifications. Cell Res **21**: 381–395.

Bates D. L., Thomas J. O., 1981 Histones H1 and H5: one or two molecules per nucleosome? Nucleic Acids Research **9**: 5883–5894.

Bednar J., Garcia-Saez I., Boopathi R., Cutter A. R., Papai G., Reymer A., Syed S. H., Lone I. N., Tonchev O., Crucifix C., Menoni H., Papin C., Skoufias D. A., Kurumizaka H., Lavery R., Hamiche A., Hayes J. J., Schultz P., Angelov D., Petosa C., Dimitrov S., 2017 Structure and Dynamics of a 197 bp Nucleosome in Complex with Linker Histone H1. Molecular Cell **66**: 384–397.e8.

Bhaumik S. R., Green M. R., 2002 Differential requirement of SAGA components for recruitment of TATA-box-binding protein to promoters in vivo. Mol. Cell. Biol. **22**: 7365–7371.

Borun T. W., Scharff M. D., Robbins E., 1967 Rapidly labeled, polyribosome-associated RNA having the properties of histone messenger. Proceedings of the National Academy of Sciences **58**: 1977–1983.

Brogaard K., Xi L., Wang J.-P., Widom J., 2012 A map of nucleosome positions in yeast at base-pair resolution. Nature **486**: 496–501.

Brown D. T., Izard T., Misteli T., 2006 Mapping the interaction surface of linker histone H10 with the nucleosome of native chromatin in vivo. Nat Struct Mol Biol **13**: 250–255.

Brownell J. E., Zhou J., Ranalli T., Kobayashi R., Edmondson D. G., Roth S. Y., Allis C. D., 1996 Tetrahymena histone acetyltransferase A: a homolog to yeast Gcn5p linking histone acetylation to gene activation. CELL **84**: 843–851.

Bustin M., Catez F., Lim J.-H., 2005 The dynamics of histone H1 function in chromatin. Molecular Cell **17**: 617–620.

Cao K., Lailler N., Zhang Y., Kumar A., Uppal K., Liu Z., Lee E. K., Wu H., Medrzycki M., Pan C., Ho P.-Y., Cooper G. P., Dong X., Bock C., Bouhassira E. E., Fan Y., 2013 High-Resolution Mapping of H1 Linker Histone Variants in Embryonic Stem Cells (WA Bickmore, Ed.). PLoS Genet **9**: e1003417–16.

Carrozza M. J., Li B., Florens L., Suganuma T., Swanson S. K., Lee K. K., Shia W.-J., Anderson S., Yates J., Washburn M. P., Workman J. L., 2005 Histone H3 Methylation by Set2 Directs Deacetylation of Coding Regions by Rpd3S to Suppress Spurious Intragenic Transcription. CELL **123**: 581–592.

Carruthers L. M., Bednar J., Woodcock C. L., Hansen J. C., 1998 Linker Histones Stabilize the Intrinsic Salt-Dependent Folding of Nucleosomal Arrays: Mechanistic Ramifications for Higher-Order Chromatin Folding †. Biochemistry **37**: 14776–14787.

Chereji R. V., Ocampo J., Clark D. J., 2017 MNase-Sensitive Complexes in Yeast: Nucleosomes and Non-histone Barriers. Molecular Cell **65**: 565–577.e3.

Chruscicki A., Macdonald V. E., Young B. P., Loewen C. J. R., Howe L. J., 2010 Critical determinants for chromatin binding by Saccharomyces cerevisiae Yng1 exist outside of the plant homeodomain finger. Genetics **185**: 469–477.

Churchman L. S., Weissman J. S., 2011 Nascent transcript sequencing visualizes transcription at nucleotide resolution. Nature **469**: 368–373.

Cieniewicz A. M., Moreland L., Ringel A. E., Mackintosh S. G., Raman A., Gilbert T. M., Wolberger C., Tackett A. J., Taverna S. D., 2014 The bromodomain of Gcn5 regulates site specificity of lysine acetylation on histone H3. Mol Cell Proteomics **13**: 2896–2910.

Clark D. J., Kimura T., 1990 Electrostatic mechanism of chromatin folding. Journal of Molecular Biology **211**: 883–896.

Clark D. J., Hill C. S., Martin S. R., Thomas J. O., 1988 Alpha-helix in the carboxy-terminal domains of histones H1 and H5. EMBO J **7**: 69–75.

Coles L. S., Robins A. J., Madley L. K., Wells J. R., 1987 Characterization of the chicken histone H1 gene complement. Generation of a complete set of vertebrate H1 protein sequences. J. Biol. Chem. **262**: 9656–9663.

Davie J. K., Edmondson D. G., Coco C. B., Dent S. Y. R., 2003 Tup1-Ssn6 interacts with multiple class I histone deacetylases in vivo. J. Biol. Chem. **278**: 50158–50162.

Dhalluin C., Carlson J. E., Zeng L., He C., Aggarwal A. K., Zhou M. M., 1999 Structure and ligand of a histone acetyltransferase bromodomain. Nature **399**: 491–496.

Dion M. F., Kaplan T., Kim M., Buratowski S., Friedman N., Rando O. J., 2007 Dynamics of replication-independent histone turnover in budding yeast. Science **315**: 1405–1408.

Downs J. A., Kosmidou E., Morgan A., Jackson S. P., 2003 Suppression of Homologous Recombination by the Saccharomyces cerevisiae Linker Histone. Molecular Cell **11**: 1685–1692.

Drouin S., Laramée L., Jacques P.-É., Forest A., Bergeron M., Robert F., 2010 DSIF and RNA Polymerase II CTD Phosphorylation Coordinate the Recruitment of Rpd3S to Actively Transcribed Genes (JD Lieb, Ed.). PLoS Genet **6**: e1001173–12.

Duggan M. M., Thomas J. O., 2000 Two DNA-binding sites on the globular domain of histone H5 are required for binding to both bulk and 5 S reconstituted nucleosomes. Journal of Molecular Biology **304**: 21–33.

Duina A. A., Winston F., 2003 Analysis of a Mutant Histone H3 That Perturbs the Association of Swi/Snf with Chromatin. Mol. Cell. Biol. **24**: 561–572.

Eriksson P. R., Ganguli D., Nagarajavel V., Clark D. J., 2012 Regulation of Histone Gene Expression in Budding Yeast. Genetics **191**: 7–20.

Fan Y., Nikitina T., Morin-Kensicki E. M., Zhao J., Magnuson T. R., Woodcock C. L., Skoultchi A. I., 2003 H1 linker histones are essential for mouse development and affect nucleosome spacing *in vivo*. Mol. Cell. Biol. **23**: 4559–4572.

Fan Y., Nikitina T., Zhao J., Fleury T. J., Bhattacharyya R., Bouhassira E. E., Stein A., Woodcock C. L., Skoultchi A. I., 2005a Histone H1 Depletion in Mammals Alters Global Chromatin Structure but Causes Specific Changes in Gene Regulation. CELL **123**: 1199–1212.

Fan Y., Nikitina T., Zhao J., Fleury T. J., Bhattacharyya R., Bouhassira E. E., Stein A., Woodcock C. L., Skoultchi A. I., 2005b Histone H1 Depletion in Mammals Alters Global Chromatin Structure but Causes Specific Changes in Gene Regulation. CELL **123**: 1199–1212.

Filippakopoulos P., Picaud S., Mangos M., Keates T., Lambert J.-P., Barsyte-Lovejoy D., Felletar I., Volkmer R., Müller S., Pawson T., Gingras A.-C., Arrowsmith C. H., Knapp S., 2012 Histone Recognition and Large-Scale Structural Analysis of the Human Bromodomain Family. CELL **149**: 214–231.

Finch J. T., Klug A., 1976 Solenoidal model for superstructure in chromatin. Proceedings of the National Academy of Sciences **73**: 1897–1901.

Freidkin I., Katcoff D. J., 2001 Specific distribution of the Saccharomyces cerevisiae linker histone homolog HHO1p in the chromatin. Nucleic Acids Research **29**: 4043–4051.

Gansen A., Tóth K., Schwarz N., Langowski J., 2009 Structural variability of nucleosomes detected by single-pair Förster resonance energy transfer: histone acetylation, sequence variation, and salt effects. J Phys Chem B **113**: 2604–2613.

Georgakopoulos T., Thireos G., 1992 Two distinct yeast transcriptional activators require the function of the GCN5 protein to promote normal levels of transcription. EMBO J **11**: 4145–4152.

Gershey E. L., Vidali G., Allfrey V. G., 1968 Chemical studies of histone acetylation. J. Biol. Chem. **243**.

Ghaemmaghami S., Huh W.-K., Bower K., Howson R. W., Belle A., Dephoure N., O'Shea E. K., Weissman J. S., 2003 Global analysis of protein expression in yeast. Nature **425**: 737–741.

Ginsburg D. S., Govind C. K., Hinnebusch A. G., 2009 NuA4 Lysine Acetyltransferase Esa1 Is Targeted to Coding Regions and Stimulates Transcription Elongation with Gcn5. Mol. Cell. Biol. **29**: 6473–6487.

Godde J. S., Ura K., 2008 Cracking the enigmatic linker histone code. J. Biochem. **143**: 287–293.

Govind C. K., Zhang F., Qiu H., Hofmeyer K., Hinnebusch A. G., 2007 Gcn5 Promotes Acetylation, Eviction, and Methylation of Nucleosomes in Transcribed Coding Regions. Molecular Cell **25**: 31–42.

Grant P. A., Duggan L., Côté J., Roberts S. M., Brownell J. E., Candau R., Ohba R., Owen-Hughes T., Allis C. D., Winston F., Berger S. L., Workman J. L., 1997 Yeast Gcn5 functions in two multisubunit complexes to acetylate nucleosomal histones: characterization of an Ada complex and the SAGA (Spt/Ada) complex. Genes & Development **11**: 1640–1650.

Grant P. A., Eberharter A., John S., Cook R. G., Turner B. M., Workman J. L., 1999 Expanded Lysine Acetylation Specificity of Gcn5 in Native Complexes. J. Biol. Chem. **274**: 5895–5900.

Gunjan A., Alexander B. T., Sittman D. B., Brown D. T., 1999 Effects of H1 Histone Variant Overexpression on Chromatin Structure. J. Biol. Chem. **274**: 37950–37956.

Happel N., Doenecke D., 2009 Histone H1 and its isoforms: Contribution to chromatin structure and function. Gene **431**: 1–12.

Happel N., Warneboldt J., Hänecke K., Haller F., Doenecke D., 2009 H1 subtype expression during cell proliferation and growth arrest. Cell Cycle **8**: 2226–2232.

Hassan A. H., Awad S., Al-Natour Z., Othman S., Mustafa F., Rizvi T. A., 2007 Selective recognition of acetylated histones by bromodomains in transcriptional co-activators. Biochem. J. **402**: 125–133.

Hebbes T. R., Thorne A. W., Crane-Robinson C., 1988 A direct link between core histone acetylation and transcriptionally active chromatin. EMBO J **7**: 1395–1402.

Hellauer K., Sirard E., Turcotte B., 2001 Decreased expression of specific genes in yeast cells lacking histone H1. J. Biol. Chem. **276**: 13587–13592.

Hendzel M. J., Lever M. A., Crawford E., Th'ng J. P. H., 2004 The C-terminal Domain Is the Primary Determinant of Histone H1 Binding to Chromatin in Vivo. J. Biol. Chem. **279**: 20028–20034.

Hong L., Schroth G. P., Matthews H. R., Yau P., Bradbury E. M., 1993 Studies of the DNA binding properties of histone H4 amino terminus. Thermal denaturation studies reveal that acetylation markedly reduces the binding constant of the H4 "tail" to DNA. J. Biol. Chem. **268**: 305–314.

Howe L., Auston D., Grant P., John S., Cook R. G., Workman J. L., Pillus L., 2001 Histone H3 specific acetyltransferases are essential for cell cycle progression. Genes & Development **15**: 3144–3154.

Hudson B. P., Martinez-Yamout M. A., Dyson H. J., Wright P. E., 2000 Solution structure and acetyl-lysine binding activity of the GCN5 bromodomain. Journal of Molecular Biology **304**: 355–370.

Human Genome Sequencing Consortium I., 2004 Finishing the euchromatic sequence of the human genome. Nature **431**: 931–945.

Hunt L. T., Dayhoff M. O., 1977 Amino-terminal sequence identity of ubiquitin and the nonhistone component of nuclear protein A24. Biochemical and Biophysical Research Communications **74**: 650–655.

Ikebe J., Sakuraba S., Kono H., 2016 H3 Histone Tail Conformation within the Nucleosome and the Impact of K14 Acetylation Studied Using Enhanced Sampling Simulation. PLoS Comput Biol **12**: e1004788.

Izzo A., Kamieniarz-Gdula K., Ramírez F., Noureen N., Kind J., Manke T., van Steensel B., Schneider R., 2013 The Genomic Landscape of the Somatic Linker Histone Subtypes H1.1 to H1.5 in Human Cells. CellReports **3**: 2142–2154.

Jiang L., Smith J. N., Anderson S. L., Ma P., Mizzen C. A., Kelleher N. L., 2007 Global assessment of combinatorial post-translational modification of core histones in yeast using contemporary mass spectrometry. LYS4 trimethylation correlates with degree of acetylation on the same H3 tail. J. Biol. Chem. **282**: 27923–27934.

John S., Howe L., Tafrov S. T., Grant P. A., Sternglanz R., Workman J. L., 2000 The something about silencing protein, Sas3, is the catalytic subunit of NuA3, a yTAF(II)30-containing HAT complex that interacts with the Spt16 subunit of the yeast CP (Cdc68/Pob3)-FACT complex. Genes & Development **14**: 1196–1208.

Joshi A. A., Struhl K., 2005 Eaf3 Chromodomain Interaction with Methylated H3-K36 Links Histone Deacetylation to Pol II Elongation. Molecular Cell **20**: 971–978.

Kadosh D., Struhl K., 1997 Repression by Ume6 Involves Recruitment of a Complex Containing Sin3 Corepressor and Rpd3 Histone Deacetylase to Target Promoters. CELL **89**: 365–371.

Kamakaka R. T., Biggins S., 2005 Histone variants: deviants? Genes & Development **19**: 295–310.

Kasinsky H. E., Lewis J. D., Dacks J. B., Ausió J., 2001 Origin of H1 linker histones. FASEB J. **15**: 34–42.

Kasten M., Szerlong H., Erdjument-Bromage H., Tempst P., Werner M., Cairns B. R., 2004 Tandem bromodomains in the chromatin remodeler RSC recognize acetylated histone H3 Lys14. EMBO J **23**: 1348–1359.

Kelley L. A., Mezulis S., Yates C. M., Wass M. N., Sternberg M. J. E., 2015 The Phyre2 web portal for protein modeling, prediction and analysis. Nature Protocols **10**: 845–858.

Kim J., Lee J., Lee T.-H., 2015 Lysine Acetylation Facilitates Spontaneous DNA Dynamics in the Nucleosome. J Phys Chem B **119**: 15001–15005.

Koutzamani E., Loborg H., Sarg B., Lindner H. H., Rundquist I., 2002 Linker histone subtype composition and affinity for chromatin in situ in nucleated mature erythrocytes. J. Biol. Chem. **277**: 44688–44694.

Kulak N. A., Pichler G., Paron I., Nagaraj N., Mann M., 2014 Minimal, encapsulated proteomic-sample processing applied to copy-number estimation in eukaryotic cells. Nat Methods **11**: 319–324.

Kuo M. H., Brownell J. E., Sobel R. E., Ranalli T. A., Cook R. G., Edmondson D. G., Roth S. Y., Allis C. D., 1996 Transcription-linked acetylation by Gcn5p of histones H3 and H4 at specific lysines. Nature **383**: 269–272.

Kurat C. F., Recht J., Radovani E., Durbic T., Andrews B., Fillingham J., 2014 Regulation of histone gene transcription in yeast. Cell. Mol. Life Sci. **71**: 599–613.

Kushnirov V. V., 2000 Rapid and reliable protein extraction from yeast. Yeast **16**: 857–860.

Landsman D., 1996 Histone H1 in Saccharomyces cerevisiae: a double mystery solved? Trends in Biochemical Sciences **21**: 287–288.

Langmead B., Salzberg S. L., 2012 Fast gapped-read alignment with Bowtie 2. Nat Methods **9**: 357–359.

Le Masson I., Yu D. Y., Jensen K., Chevalier A., Courbeyrette R., Boulard Y., Smith M. M., Mann C., 2003 Yaf9, a novel NuA4 histone acetyltransferase subunit, is required for the cellular response to spindle stress in yeast. Mol. Cell. Biol. **23**: 6086–6102.

Lee D. Y., Hayes J. J., Pruss D., Wolffe A. P., 1993 A positive role for histone acetylation in transcription factor access to nucleosomal DNA. CELL **72**: 73–84.

Li B., Jackson J., Simon M. D., Fleharty B., Gogol M., Seidel C., Workman J. L., Shilatifard A., 2009 Histone H3 lysine 36 dimethylation (H3K36me2) is sufficient to recruit the Rpd3s histone deacetylase complex and to repress spurious transcription. J. Biol. Chem. **284**: 7970–7976.

Li J.-Y., Patterson M., Mikkola H. K. A., Lowry W. E., Kurdistani S. K., 2012 Dynamic distribution of linker histone H1.5 in cellular differentiation. (HD Madhani, Ed.). PLoS Genet **8**: e1002879.

Li M., Valsakumar V., Poorey K., Bekiranov S., Smith J. S., 2013 Genome-wide analysis of functional sirtuin chromatin targets in yeast. Genome Biol. **14**: R48.

Li W., Nagaraja S., Delcuve G. P., Hendzel M. J., Davie J. R., 1993 Effects of histone acetylation, ubiquitination and variants on nucleosome stability. Biochem. J. **296** : 737–744.

Li Y., Wen H., Xi Y., Tanaka K., Wang H., Peng D., Ren Y., Jin Q., Dent S. Y. R., Li W., Li H., Shi X., 2014 AF9 YEATS domain links histone acetylation to DOT1L-mediated H3K79 methylation. CELL **159**: 558–571.

Lifton R. P., Goldberg M. L., Karp R. W., Hogness D. S., 1978 The Organization of the Histone Genes in Drosophila melanogaster: Functional and Evolutionary Implications. Cold Spring Harb. Symp. Quant. Biol. **42**: 1047–1051.

Liu C. L., Kaplan T., Kim M., Buratowski S., Schreiber S. L., Friedman N., Rando O. J., 2005a Single-Nucleosome Mapping of Histone Modifications in S. cerevisiae (P Becker, Ed.). PLoS Biol **3**: e328–17.

Liu C. L., Kaplan T., Kim M., Buratowski S., Schreiber S. L., Friedman N., Rando O. J., 2005b Single-nucleosome mapping of histone modifications in S. cerevisiae. PLoS Biol **3**: e328.

Lohe A. R., Hilliker A. J., Roberts P. A., 1993 Mapping Simple Repeated DNA Sequences in Heterochromatin of Drosophila melanogaster. Genetics **134**: 1149–1174.

Luger K., Richmond T. J., 1998 The histone tails of the nucleosome. Curr. Opin. Genet. Dev. **8**: 140–146.

Luger K., Mäder A. W., Richmond R. K., Sargent D. F., Richmond T. J., 1997 Crystal structure of the nucleosome core particle at 2.8 A resolution. Nature **389**: 251–260.

Maeshima K., Hihara S., Eltsov M., 2010 Chromatin structure: does the 30-nm fibre exist in vivo? Curr. Opin. Cell Biol. **22**: 291–297.

Malavé T. M., Dent S. Y. R., 2006 Transcriptional repression by Tup1-Ssn6. Biochem. Cell Biol. **84**: 437–443.

Maltby V. E., Martin B. J. E., Brind'Amour J., Chruscicki A. T., McBurney K. L., Schulze J. M., Johnson I. J., Hills M., Hentrich T., Kobor M. S., Lorincz M. C., Howe L. J., 2012a Histone H3K4 demethylation is negatively regulated by histone H3 acetylation in Saccharomyces cerevisiae. Proceedings of the National Academy of Sciences **109**: 18505–18510.

Maltby V. E., Martin B. J. E., Schulze J. M., Johnson I., Hentrich T., Sharma A., Kobor M. S., Howe L., 2012b Histone H3 Lysine 36 Methylation Targets the Isw1b Remodeling Complex to Chromatin. Mol. Cell. Biol. **32**: 3479–3485.

Martin B. J. E., McBurney K. L., Maltby V. E., Jensen K. N., Brind'Amour J., Howe L. J., 2017 Histone H3K4 and H3K36 Methylation Independently Recruit the NuA3 Histone Acetyltransferase in Saccharomyces cerevisiae. Genetics **205**: 1113–1123.

Martin D. G. E., Baetz K., Shi X., Walter K. L., MacDonald V. E., Wlodarski M. J., Gozani O., Hieter P., Howe L., 2006 The Yng1p Plant Homeodomain Finger Is a Methyl-Histone Binding Module That Recognizes Lysine 4-Methylated Histone H3. Mol. Cell. Biol. **26**: 7871–7879.

Marzluff W. F., Gongidi P., Woods K. R., Jin J., Maltais L. J., 2002 The Human and Mouse Replication-Dependent Histone Genes. Genomics **80**: 487–498.

Maze I., Noh K.-M., Soshnev A. A., Allis C. D., 2014 Every amino acid matters: essential contributions of histone variants to mammalian development and disease. Nat Rev Genet **15**: 259–271.

Meyer S., Becker N. B., Syed S. H., Goutte-Gattat D., Shukla M. S., Hayes J. J., Angelov D., Bednar J., Dimitrov S., Everaers R., 2011 From crystal and NMR structures, footprints and cryo-electron-micrographs to large and soft structures: nanoscale modeling of the nucleosomal stem. Nucleic Acids Research **39**: 9139–9154.

Millán-Ariño L., Islam A. B. M. M. K., Izquierdo-Bouldstridge A., Mayor R., Terme J.-M., Luque N., Sancho M., López-Bigas N., Jordan A., 2014 Mapping of six somatic linker histone H1 variants in human breast cancer cells uncovers specific features of H1.2. Nucleic Acids Research **42**: 4474–4493.

Misteli T., Gunjan A., Hock R., Bustin M., Brown D. T., 2000 Dynamic binding of histone H1 to chromatin in living cells. Nature **408**: 877–881.

Morales V., Richard-Foy H., 2000 Role of Histone N-Terminal Tails and Their Acetylation in Nucleosome Dynamics. Mol. Cell. Biol. **20**: 7230–7237.

Mumberg D., Muller R., Funk M., 1994 Regulatable promoters of Saccharomyces cerevisiae: comparison of transcriptional activity and their use for heterologous expression. Nucleic Acids Research **22**: 5767–5768.

Murray K., 1964 The Occurrence of ε-N-Methyl Lysine in Histones. Biochemistry **3**: 10–15.

Nalabothula N., McVicker G., Maiorano J., Martin R., Pritchard J. K., Fondufe-Mittendorf Y. N., 2014 The chromatin architectural proteins HMGD1 and H1 bind reciprocally and have opposite effects on chromatin structure and gene regulation. BMC Genomics **15**: 92.

Neumann H., Hancock S. M., Buning R., Routh A., Chapman L., Somers J., Owen-Hughes T., van Noort J., Rhodes D., Chin J. W., 2009 A method for genetically installing site-specific acetylation in recombinant histones defines the effects of H3 K56 acetylation. Molecular Cell **36**: 153–163.

Norton V. G., Imai B. S., Yau P., Bradbury E. M., 1989 Histone acetylation reduces nucleosome core particle linking number change. CELL **57**: 449–457.

Obrdlik A., Kukalev A., Louvet E., Ostlund Farrants A. K., Caputo L., Percipalle P., 2008 The Histone Acetyltransferase PCAF Associates with Actin and hnRNP U for RNA Polymerase II Transcription. Mol. Cell. Biol. **28**: 6342–6357.

Ocampo J., Chereji R. V., Eriksson P. R., Clark D. J., 2016 The ISW1 and CHD1 ATP-dependent chromatin remodelers compete to set nucleosome spacing in vivo. Nucleic Acids Research **44**: 4625–4635.

Ono K., Kusano O., Shimotakahara S., Shimizu M., Yamazaki T., Shindo H., 2003 The linker histone homolog Hho1p from Saccharomyces cerevisiae represents a winged helix-turn-helix fold as determined by NMR spectroscopy. Nucleic Acids Research **31**: 7199–7207.

Owen D. J., 2000 The structural basis for the recognition of acetylated histone H4 by the bromodomain of histone acetyltransferase Gcn5p. EMBO J **19**: 6141–6149.

Patterton H. G., Landel C. C., Landsman D., Peterson C. L., Simpson R. T., 1998 The Biochemical and Phenotypic Characterization of Hho1p, the Putative Linker Histone H1 of Saccharomyces cerevisiae. J. Biol. Chem. **273**: 7268–7276.

Pettersen E. F., Goddard T. D., Huang C. C., Couch G. S., Greenblatt D. M., Meng E. C., Ferrin T. E., 2004 UCSF Chimera - A Visualization System for Exploratory Research and Analysis. J Comput Chem **25**: 1605–1612.

Pérez-Montero S., Carbonell A., Morán T., Vaquero A., Azorín F., 2013 The Embryonic Linker Histone H1 Variant of Drosophila, dBigH1, Regulates Zygotic Genome Activation. Developmental Cell **26**: 578–590.

Phillips D. M., 1963 The presence of acetyl groups of histones. Biochem. J. **87**: 258–263.

Pokholok D. K., Harbison C. T., Levine S., Cole M., Hannett N. M., Lee T. I., Bell G. W., Walker K., Rolfe P. A., Herbolsheimer E., Zeitlinger J., Lewitter F., Gifford D. K., Young R. A., 2005 Genome-wide map of nucleosome acetylation and methylation in yeast. CELL **122**: 517–527.

Ponte I., 2003 Sequence Complexity of Histone H1 Subtypes. Molecular Biology and Evolution **20**: 371–380.

Pray-Grant M. G., Schieltz D., McMahon S. J., Wood J. M., Kennedy E. L., Cook R. G., Workman J. L., Yates J. R., Grant P. A., 2002 The novel SLIK histone acetyltransferase complex functions in the yeast retrograde response pathway. Mol. Cell. Biol. **22**: 8774–8786.

Raghuram N., Carrero G., Stasevich T. J., McNally J. G., Th'ng J., Hendzel M. J., 2010 Core histone hyperacetylation impacts cooperative behavior and high-affinity binding of histone H1 to chromatin. Biochemistry **49**: 4420–4431.

Ramakrishnan V., Finch J. T., Graziano V., Lee P. L., Sweet R. M., 1993 Crystal structure of globular domain of histone H5 and its implications for nucleosome binding. Nature **362**: 219–223.

Ramírez F., Dündar F., Diehl S., Grüning B. A., Manke T., 2014 deepTools: a flexible platform for exploring deep-sequencing data. Nucleic Acids Research **42**: W187–W191.

Ramírez F., Ryan D. P., Grüning B., Bhardwaj V., Kilpert F., Richter A. S., Heyne S., Dündar F., Manke T., 2016 deepTools2: a next generation web server for deep-sequencing data analysis. Nucleic Acids Research **44**: W160–W165.

Ravindra A., Weiss K., Simpson R. T., 1999 High-Resolution Structural Analysis of Chromatin at Specific Loci: Saccharomyces cerevisiae Silent Mating-Type Locus HMRa. Mol. Cell. Biol. **19**: 7944–7950.

Rhee H. S., Bataille A. R., Zhang L., Pugh B. F., 2014 Subnucleosomal Structures and Nucleosome Asymmetry across a Genome. CELL **159**: 1377–1388.

Ricci M. A., Manzo C., García-Parajo M. F., Lakadamyali M., Cosma M. P., 2015 Chromatin fibers are formed by heterogeneous groups of nucleosomes in vivo. CELL **160**: 1145–1158.

Robert F., Pokholok D. K., Hannett N. M., Rinaldi N. J., Chandy M., Rolfe A., Workman J. L., Gifford D. K., Young R. A., 2004 Global Position and Recruitment of HATs and HDACs in the Yeast Genome. Molecular Cell **16**: 199–209.

Robinson P. J. J., Rhodes D., 2006 Structure of the "30 nm" chromatin fibre: a key role for the linker histone. Current Opinion in Structural Biology **16**: 336–343.

Robinson P. J. J., An W., Routh A., Martino F., Chapman L., Roeder R. G., Rhodes D., 2008 30 nm chromatin fibre decompaction requires both H4-K16 acetylation and linker histone eviction. Journal of Molecular Biology **381**: 816–825.

Robinson P. J. J., Fairall L., Huynh V. A. T., Rhodes D., 2006 EM measurements define the dimensions of the "30-nm" chromatin fiber: evidence for a compact, interdigitated structure. Proceedings of the National Academy of Sciences **103**: 6506–6511.

Routh A., Sandin S., Rhodes D., 2008 Nucleosome repeat length and linker histone stoichiometry determine chromatin fiber structure. Proc. Natl. Acad. Sci. U.S.A. **105**: 8872–8877.

Rufiange A., Jacques P.-É., Bhat W., Robert F., Nourani A., 2007 Genome-Wide Replication-Independent Histone H3 Exchange Occurs Predominantly at Promoters and Implicates H3 K56 Acetylation and Asf1. Molecular Cell **27**: 393–405.

Rundlett S. E., Carmen A. A., Suka N., Turner B. M., Grunstein M., 1998 Transcriptional repression by UME6 involves deacetylation of lysine 5 of histone H4 by RPD3. Nature **392**: 831–835.

Rusche L. N., Kirchmaier A. L., Rine J., 2003 The establishment, inheritance, and function of silenced chromatin in Saccharomyces cerevisiae. Annu. Rev. Biochem. **72**: 481–516.

Sarma K., Reinberg D., 2005 Histone variants meet their match. Nat Rev Mol Cell Biol **6**: 139–149.

Schafer G., McEvoy C. R. E., Patterton H. G., 2008 The Saccharomyces cerevisiae linker histone Hho1p is essential for chromatin compaction in stationary phase and is displaced by transcription. Proceedings of the National Academy of Sciences **105**: 14838–14843.

Schäfer G., Smith E. M., Patterton H. G., 2005 The Saccharomyces cerevisiae Linker Histone Hho1p, with Two Globular Domains, Can Simultaneously Bind to Two Four-Way Junction DNA Molecules. Biochemistry **44**: 16766–16775.

Sendra R., Tse C., Hansen J. C., 2000 The yeast histone acetyltransferase A2 complex, but not free Gcn5p, binds stably to nucleosomal arrays. J. Biol. Chem. **275**: 24928–24934.

Shen X., Gorovsky M. A., 1996 Linker histone H1 regulates specific gene expression but not global transcription *in vivo*. CELL **86**: 475–483.

Shen X., Yu L., Weir J. W., Gorovsky M. A., 1995 Linker histones are not essential and affect chromatin condensation in vivo. CELL **82**: 47–56.

Shi X., Hong T., Walter K. L., Ewalt M., Michishita E., Hung T., Carney D., Peña P., Lan F., Kaadige M. R., Lacoste N., Cayrou C., Davrazou F., Saha A., Cairns B. R., Ayer D. E.,

Kutateladze T. G., Shi Y., Cote J., Chua K. F., Gozani O., 2006 ING2 PHD domain links histone H3 lysine 4 methylation to active gene repression. Nature **442**: 96–99.

Shi X., Kachirskaia I., Walter K. L., Kuo J.-H. A., Lake A., Davrazou F., Chan S. M., Martin D. G. E., Fingerman I. M., Briggs S. D., Howe L., Utz P. J., Kutateladze T. G., Lugovskoy A. A., Bedford M. T., Gozani O., 2007 Proteome-wide analysis in Saccharomyces cerevisiae identifies several PHD fingers as novel direct and selective binding modules of histone H3 methylated at either lysine 4 or lysine 36. J. Biol. Chem. **282**: 2450–2455.

Shogren-Knaak M., 2006 Histone H4-K16 Acetylation Controls Chromatin Structure and Protein Interactions. Science **311**: 844–847.

Shogren-Knaak M., Ishii H., Sun J.-M., Pazin M. J., Davie J. R., Peterson C. L., 2006 Histone H4-K16 acetylation controls chromatin structure and protein interactions. Science **311**: 844–847.

Simon M., North J. A., Shimko J. C., Forties R. A., Ferdinand M. B., Manohar M., Zhang M., Fishel R., Ottesen J. J., Poirier M. G., 2011 Histone fold modifications control nucleosome unwrapping and disassembly. Proc. Natl. Acad. Sci. U.S.A. **108**: 12711–12716.

Singer D. S., Singer M. F., 1976 Studies on the interaction of H1 histone with superhelical DNA: characterization of the recognition and binding regions of H1 histones. Nucleic Acids Research **3**: 2531–2547.

Smith J. S., Burke D. J. (Eds.), 2014 *Yeast Genetics*. Springer New York, New York, NY.

Smith P. A., Jackson V., Chalkley R., 1984 Two-stage maturation process for newly replicated chromatin. Biochemistry **23**: 1576–1581.

Song F., Chen P., Sun D., Wang M., Dong L., Liang D., Xu R.-M., Zhu P., Li G., 2014 Cryo-EM study of the chromatin fiber reveals a double helix twisted by tetranucleosomal units. Science **344**: 376–380.

Spalding J., Kajiwara K., Mueller G. C., 1966 The metabolism of basic proteins in HeLa cell nuclei. Proceedings of the National Academy of Sciences **56**: 1535–1542.

Spellman P. T., Sherlock G., Zhang M. Q., Iyer V. R., Anders K., Eisen M. B., Brown P. O., Botstein D., Futcher B., 1998 Comprehensive identification of cell cycle-regulated genes of the yeast *Saccharomyces cerevisiae* by microarray hybridization. Molecular Biology of the Cell **9**: 3273–3297.

Stedman E., Stedman E., 1951 The Basic Proteins of Cell Nuclei. Philosophical Transactions of the Royal Society **235**: 565–595.

Stevely W. S., Stocken L. A., 1966 Phosphorylation of rat-thymus histone. Biochem. J. **100**: 20C–1C.

Strahl B. D., Allis C. D., 2000 The language of covalent histone modifications. Nature **403**: 41–45.

Struhl K., 1998 Histone acetylation and transcriptional regulatory mechanisms. Genes & Development **12**: 599–606.

Su D., Hu Q., Li Q., Thompson J. R., Cui G., Fazly A., Davies B. A., Botuyan M. V., Zhang Z., Mer G., 2012 Structural basis for recognition of H3K56-acetylated histone H3-H4 by the chaperone Rtt106. Nature **483**: 104–107.

Suka N., Suka Y., Carmen A. A., Wu J., Grunstein M., 2001 Highly Specific Antibodies Determine Histone Acetylation Site Usage in Yeast Heterochromatin and Euchromatin. Molecular Cell **8**: 473–479.

Suto R. K., Clarkson M. J., Tremethick D. J., Luger K., 2000 Crystal structure of a nucleosome core particle containing the variant histone H2A.Z. Nat. Struct. Biol. **7**: 1121–1124.

Syed S. H., Goutte-Gattat D., Becker N., Meyer S., Shukla M. S., Hayes J. J., Everaers R., Angelov D., Bednar J., Dimitrov S., 2010 Single-base resolution mapping of H1-nucleosome interactions and 3D organization of the nucleosome. Proceedings of the National Academy of Sciences **107**: 9620–9625.

Szilard R. K., Jacques P.-É., Laramée L., Cheng B., Galicia S., Bataille A. R., Yeung M., Mendez M., Bergeron M., Robert F., Durocher D., 2010 Systematic identification of fragile sites via genome-wide location analysis of gamma-H2AX. Nature Publishing Group **17**: 299–305.

Takechi S., Nakayama T., 1999 Sas3 is a histone acetyltransferase and requires a zinc finger motif. Biochemical and Biophysical Research Communications **266**: 405–410.

Talbert P. B., Henikoff S., 2010 Histone variants - ancient wrap artists of the epigenome. Nat Rev Mol Cell Biol **11**: 264–275.

Taunton J., Hassig C. A., Schreiber S. L., 1996 A mammalian histone deacetylase related to the yeast transcriptional regulator Rpd3p. Science **272**: 408–411.

Thoma F., Koller T., 1981 Unravelled nucleosomes, nucleosome beads and higher order structures of chromatin: Influence of non-histone components and histone H1. Journal of Molecular Biology **149**: 709–733.

Thoma F., Koller T., Klug A., 1979 Involement of histon H1 in the organization of the nucleosome and of the salt-dependent structures of chromatin. The Journal of Cell Biology **83**: 403–427.

Tse C., Sera T., Wolffe A. P., Hansen J. C., 1998 Disruption of higher-order folding by core histone acetylation dramatically enhances transcription of nucleosomal arrays by RNA polymerase III. Mol. Cell. Biol. **18**: 4629–4638.

Ushinsky S. C., Bussey H., Ahmed A. A., Wang Y., Friesen J., Williams B. A., Storms R. K., 1997 Histone H1 in *Saccharomyces cerevisiae*. Yeast **13**: 151–161.

Valero M. L., Sendra R., Pamblanco M., 2016 Tandem affinity purification of histones, coupled to mass spectrometry, identifies associated proteins and new sites of post-translational modification in Saccharomyces cerevisiae. J Proteomics **136**: 183–192.

van Bakel H., Tsui K., Gebbia M., Mnaimneh S., Hughes T. R., Nislow C., 2013 A compendium of nucleosome and transcript profiles reveals determinants of chromatin architecture and transcription. PLoS Genet **9**: e1003479.

van Holde K. E., 1989 *Chromatin* (A Rich, Ed.). Springer-Verlag, New York, NY.

Wakamori M., Fujii Y., Suka N., Shirouzu M., Sakamoto K., Umehara T., Yokoyama S., 2015 Intra- and inter-nucleosomal interactions of the histone H4 tail revealed with a human nucleosome core particle with genetically-incorporated H4 tetra-acetylation. Nature Publishing Group **5**: 17204.

Wang X., Hayes J. J., 2008 Acetylation mimics within individual core histone tail domains indicate distinct roles in regulating the stability of higher-order chromatin structure. Mol. Cell. Biol. **28**: 227–236.

Wang Z., Zang C., Rosenfeld J. A., Schones D. E., Barski A., Cuddapah S., Cui K., Roh T.-Y., Peng W., Zhang M. Q., Zhao K., 2008 Combinatorial patterns of histone acetylations and methylations in the human genome. Nat Genet **40**: 897–903.

Weiner A., Chen H. V., Liu C. L., Rahat A., Klien A., Soares L., Gudipati M., Pfeffner J., Regev A., Buratowski S., Pleiss J. A., Friedman N., Rando O. J., 2012 Systematic Dissection of Roles for Chromatin Regulators in a Yeast Stress Response (J Workman, Ed.). PLoS Biol **10**: e1001369–20.

Weiner A., Hsieh T.-H. S., Appleboim A., Chen H. V., Rahat A., Amit I., Rando O. J., Friedman N., 2015 High-Resolution Chromatin Dynamics during a Yeast Stress Response. Molecular Cell **58**: 371–386.

Weiss K., Simpson R. T., 1998 High-resolution structural analysis of chromatin at specific loci: Saccharomyces cerevisiae silent mating type locus HMLalpha. Mol. Cell. Biol. **18**.

Wiśniewski J. R., Zougman A., Krüger S., Mann M., 2007 Mass Spectrometric Mapping of Linker Histone H1 Variants Reveals Multiple Acetylations, Methylations, and

Phosphorylation as Well as Differences between Cell Culture and Tissue. Mol Cell Proteomics **6**: 72–87.

Woodcock C. L., Skoultchi A. I., Fan Y., 2006 Role of linker histone in chromatin structure and function: H1 stoichiometry and nucleosome repeat length. Chromosome Res **14**: 17–25.

Wu J., Suka N., Carlson M., Grunstein M., 2001 TUP1 Utilizes Histone H3/H2B–Specific HDA1 Deacetylase to Repress Gene Activity in Yeast. Molecular Cell **7**: 117–126.

Young B. P., Loewen C. J., 2013 Balony: a software package for analysis of data generated by synthetic genetic array experiments. BMC Bioinformatics **14**: 354–17.

Yu Q., Kuzmiak H., Zou Y., Olsen L., Defossez P.-A., Bi X., 2009 Saccharomyces cerevisiaeLinker Histone Hho1p Functionally Interacts with Core Histone H4 and Negatively Regulates the Establishment of Transcriptionally Silent Chromatin. J. Biol. Chem. **284**: 740–750.

Zeng L., Zhang Q., Li S., Plotnikov A. N., Walsh M. J., Zhou M.-M., 2010 Mechanism and regulation of acetylated histone binding by the tandem PHD finger of DPF3b. Nature **466**: 258–262.

Zhang L., Eugeni E. E., Parthun M. R., Freitas M. A., 2003 Identification of novel histone post-translational modifications by peptide mass fingerprinting. Chromosoma **112**: 77–86.

Zhang L., Ma H., Pugh B. F., 2011 Stable and dynamic nucleosome states during a meiotic developmental process. Genome Research **21**: 875–884.

Zhao Y., Garcia B. A., 2015 Comprehensive Catalog of Currently Documented Histone Modifications. Cold Spring Harb Perspect Biol **7**: a025064.

Zhou B. R., Feng H., Kato H., Dai L., Yang Y., Zhou Y., Bai Y., 2013 Structural insights into the histone H1-nucleosome complex. Proceedings of the National Academy of Sciences **110**: 19390–19395.

Zhou B.-R., Feng H., Ghirlando R., Li S., Schwieters C. D., Bai Y., 2016 A Small Number of Residues Can Determine if Linker Histones Are Bound On or Off Dyad in the Chromatosome. Journal of Molecular Biology **428**: 3948–3959.

Zhou B.-R., Jiang J., Feng H., Ghirlando R., Xiao T. S., Bai Y., 2015a Structural Mechanisms of Nucleosome Recognition by Linker Histones. Molecular Cell **59**: 628–638.

Zhou B.-R., Jiang J., Feng H., Ghirlando R., Xiao T. S., Bai Y., 2015b Structural Mechanisms of Nucleosome Recognition by Linker Histones. Molecular Cell **59**: 628–638.

Zhou Y. B., Gerchman S. E., Ramakrishnan V., Travers A., Muyldermans S., 1998 Position and orientation of the globular domain of linker histone H5 on the nucleosome. Nature **395**: 402–405.

Zlatanova J., Doenecke D., 1994 Histone H1^{o}: a major player in cell differentiation? FASEB J. **8**: 1260–1268.